Structure-Acoustic Analysis; Methods, implementations and applications

Wernberg, Per-Anders

2006

Document Version:
Publisher's PDF, also known as Version of record

LUND UNIVERSITY

STRUCTURE-ACOUSTIC ANALYSIS
Methods, Implementations and Applications

PER-ANDERS WERNBERG

Structural
Mechanics

Doctoral Thesis

Department of Construction Sciences
Structural Mechanics

ISRN LUTVDG/TVSM--06/1019--SE (1-116)
ISBN 91-628-6888-8 ISSN 0281-6679

STRUCTURE-ACOUSTIC ANALYSIS
Methods, Implementations and Applications

Doctoral Thesis by

PER-ANDERS WERNBERG

Printed by KFS i Lund AB, Lund, Sweden, May 2006.

For information, address:
Division of Structural Mechanics, LTH, Lund University, Box 118, SE-221 00 Lund, Sweden.
Homepage: http://www.byggmek.lth.se

To Anna,
Olivia, Arvid and Adam

Preface

The work presented in this thesis has been carried out at the Division of Structural Mechanics at Lund University. I would like to express my gratitude to my supervisor Professor Göran Sandberg, for his support and encouragement during this work The friendship and support of all colleagues at the division are very appreciated. A special thanks to Mr. Bo Zadig for the help on creating a variety of the figures and to Professor Ola Dahlblom for proofreading of the original manuscript and for valuable comments.

The latter part of this thesis was a result of participation in the research school "The building an its indoor environment" at Lund University. This research school was financed through KK-stiftelsen (The Swedish Foundation for Knowledge and Competence Development). This is gratefully acknowledged.

Finally, I wish to express my deepest gratitude to my family, parents and friends for all their love and support throughout the course of this work.

Lund, May 2006

Per-Anders Wernberg

Overview of the thesis

This thesis investigates structure-acoustic problems, which involve a flexible structure coupled to an enclosed acoustic fluid. In the literature, this type of problem is usually referred to as vibroacoustic problems or structure-acoustic problems with fluid interaction. The thesis consists of two parts. The first part provides an introduction into the field of structure-acoustic analysis within the finite element framework. The second part of the thesis comprises six papers in which analysis procedures and application examples for structure-acoustic systems are developed.

Included papers

Paper 1 P-A. Hansson[1], and G. Sandberg, Mass matrices by minimization of modal errors, *International Journal for Numerical Methods in Engineering*, **40**, 4259-4271(1997)

Paper 2 G. Sandberg, P-A. Hansson[1], M. Gustavsson, Domain Decomposition in Acoustic and Structure-Acoustic Analysis, *Computer methods in applied mechanics and engineering*, **190**, 2979-2988(2001)

Paper 3 P-A. Wernberg, G. Sandberg, A symmetric time-stepping scheme for coupled problems, *WCCM V congress in Vienna*, 2002.

Paper 4 P-A. Hansson[1] and G. Sandberg, Dynamic Finite Element Analysis of Fluid-filled Pipes, *Computer methods in applied mechanics and engineering*, **190**, 3111-3120(2001)

Paper 5 P. Davidsson, J. Brunskog, P-A. Wernberg, G. Sandberg and P. Hammer, Analysis of sound transmission loss of double-leaf walls in the low-frequency range using the finite element method, *Building Acoustics*, **11**, 239-257(2004)

Paper 6 P-A. Wernberg, G. Sandberg, The Finite Element Method as a design instrument for room acoustical environment., Report TVSM-7144, Division of Structural Mechanics, Lund University,(2006)

[1]Name changed to P-A Wernberg due to marriage.

Summary of papers

Paper 1 A new approach to constructing mass matrices is presented, based on use of a variable parameter. This allows the mass matrix to be adjusted in such a way that a simple eigenvalue problem gets the best solution possible in terms of some error measure. This procedure is used to create both diagonal mass matrices and mixed mass matrices.

Paper 2 Finite element analysis in acoustics, structure-acoustics, and structure-hydro-acoustic engineering applications leads to large systems of equations, and is still a challenge to current high performance computer systems. The demands for extremely large models are due to large physical domains or the desire to resolve high frequency levels, at least as long as the different modes are separated, say to 500 Hz. This obviously calls for small elements. It is therefore of great interest to have procedures for domain splitting, fluid-structure and fluid-fluid, thus splitting the analysis procedure into smaller problems. Use of multiple processing also lies down the road. Furthermore changes in design often affect only part of the geometry, thus, only that particular domain needs to be recalculated, for instance in the case of sound quality engineering. The interest and efforts put into numerical methods related to fluid-structure interaction are still spreading. This applies both to engineering application studies and applied mathematical issues related to the topic. A reduction procedure of the structure and multiple fluid domains is exercised. The coupled problem is formulated as a symmetric standard problem. A subsequent analysis in the time domain can be performed on a subset of the eigenmodes.

Paper 3 In a particular class of coupled problems, the resulting coupled set of equations is unsymmetrical. In this paper a simple procedure for introducing a symmetric effective stiffness matrix using implicit time stepping procedures in fluid-structure problems, is proposed. As long as the time step is kept constant, the factorization of the effective stiffness matrix only needs to be performed once. The numerical example shows that cpu time and memory utilization decrease with the proposed formulation.

Paper 4 A finite element model for studying fluid-filled pipes is developed by combining an axisymmetric shell element and a one-dimensional fluid element and taking the interaction between shell and fluid into account. Both a symmetric and an unsymmetric element have been developed and evaluated numerically.

Paper 5 The sound transmission loss of double-leaf walls in the low-frequency range is evaluated by means of structure-acoustic finite element analysis. A parametric study is performed to investigate the influence on the sound transmission loss of various material and geometric properties of the wall and the dimensions of the connecting rooms. It is found that a very detailed description of the system is needed in order to describe sound transmission loss in the low-frequency range. The model confirms the importance of primary structural resonance and the size of the wall and the connecting rooms in determining the sound transmission loss in the low-frequency range.

Paper 6 Room acoustic design is an important area to study. It affects many people's daily life, especially with the increasing number of sources of noise. This paper discusses how tools like the finite element method could be used in the low frequency range to improve designs. The fact that the geometric description of the structure could be very exact, and also modified easily in the model, makes it an attractive tool in the design process. Combined with theories for how stochastic variables could be incorporated in the analysis, a discussion about how these techniques could be used is conducted through a couple of application examples. The result is not a complete tool, ready to be used, but the start of discussion of how such a tool could look like.

Contents

Preface **I**

Overview of the thesis **III**
Included papers . . . III
Summary of papers . . . V

Contents **VII**

1 Introduction **1**
1.1 Background . . . 1
1.2 Objective . . . 2
1.3 Problem description . . . 2
1.4 The development of this thesis . . . 2

2 Structure-acoustic analysis **5**
2.1 Literature review . . . 5
2.2 Governing equations and finite element formulation . . . 7
2.2.1 Acoustic fluid domain . . . 7
2.2.2 Boundary terms . . . 9
2.2.3 Structural domain . . . 9
2.2.4 The coupled structure-acoustic system . . . 11
2.3 Mass lumping . . . 13
2.3.1 Introduction. . . . 13
2.3.2 Consistent and non-consistent mass matrices. . . . 13
2.3.3 Mass lumping by nodal quadrature . . . 14
2.3.4 Row-sum technique . . . 15
2.3.5 Special lumping technique . . . 15
2.3.6 Consistent diagonal mass matrix . . . 16
2.3.7 Mixed mass matrices. . . . 17
2.3.8 Freqency dependent mass matrices. . . . 17
2.4 Dynamic analysis of piping systems . . . 20
2.4.1 Introduction. . . . 20
2.4.2 Transient analysis of fluid-filled pipes. . . . 22

3 Concluding Remarks and Contributions **23**

Bibliography **25**

Included papers

Chapter 1

Introduction

This thesis treats simulation of structure-acoustic systems. The introduction gives the background and objective for the thesis and also describes a number of applications where this type of analysis can be employed. The typical procedure of structure-acoustic analysis is discussed, including the generation of the governing system of equations.

The introduction also contains a description of the work conducted, as based on the included papers where the main contributions of the included papers to this thesis are stated.

The next chapter contains a short theoretical introduction to the basic equation involved, as well as a more detailed background to the theories about the analysis procedures in some of the papers.

In the third chapter some concluding remarks and future prospects are given.

1.1 Background

Situations where acoustic and structure-acoustic analysis is of great importance are found in a number of applications. First, to define the term structure acoustic analysis, one usually refers to problems where the behaviour of the acoustic domain is influenced by the structure, and vice versa, the structural behaviour is influenced by the acoustic domain. The problem is said to be coupled, in opposite to e.g. an acoustic problem, where the structural vibrations are imposed to the acoustic domain as a boundary condition.

Two common applications for acoustic and structure-acoustic analysis is the passenger compartments in automobiles and aircraft. The increased use of light-weight materials in these vehicles usually makes it even more complicated to achieve good passenger comfort in terms of low level of interior noise. When the weight of the structure is reduced, the dynamic vibrations could be increased and that could lead to higher noise levels. Other applications where structure acoustic analysis is of interest is in light-weight constructions of buildings and in mobile phones, to mention but a few.

In all these situations the designer wants be able to predict the acoustic behavior of the product at an early design stage. To be able to do so, numerical analysis of the structure acoustic equations has to be conducted. The most commonly used method in these situations is the finite element method.

The interior noise comfort, or the acoustic performance of a speaker in a mobile phone is often in conflict with other important aspects of the product. In the car case it could be e.g. crashworthiness and in case of the mobile phone it could be space or rather lack of space. In these complex design situations it is very important to have accurate and efficient numerical tools that can help the engineers to test different designs and to find a good solution.

1.2 Objective

In this thesis, the coupled structure-acoustic problem is studied using the finite element method. The systems studied here are limited to those that consist of an enclosed acoustic fluid cavity, which is coupled to a flexible structure. The objective is twofold: to develop the analysis methods and to study engineering applications.

An important aspect of structure-acoustic analysis is that the number of degrees of freedom often becomes very large. This is mainly due to the fact that the wavelengths of the acoustic fluid and structure must be properly resolved in the finite element model. At higher frequencies the wavelength becomes very short and that in turn leads to very small elements to be able to resolve this short wavelength. This, and the fact that the structure-acoustic system is unsymmetric in the most simple formulation, calls for better solution strategies and decomposition methods.

Anther goal of this thesis is to use the derived procedures in engineering applications. In the last part of the thesis room acoustical problems are studied. Sound transmission loss of lightweight double-leaf walls in the lower frequency range are studied. The objective is to include all the geometric details of the structure and to see how different configurations of the structure influences on the sound transmission loss. The last paper discusses the possibility to use the finite element method as a tool in room acoustic design. The objective is to discuss possible scenarios where room acoustical modelling could benefit from using the finite element method.

1.3 Problem description

Finite element analysis of structure-acoustic systems is applicable to a wide range of engineering problems. Some of these applications will be illustrated here. Figure 1.1 shows results from an analysis of a room with flexible walls from Paper 2. The results are from both a full system and a reduced system. The example from this paper shows that with the reduction technique presented the model can be substantially reduced without too much deterioration in the results. Another example is an analysis of a pipe from Paper 4. The problem is reduced to an axisymmetric model, leading to a great reduction in model size.

A third example is from a building acoustic application. Figure 1.3 shows an analysis of a double room with a flexible wall that divides the room from Paper 5. The analysis is a fully coupled structure-acoustic analysis, but a reduction technique has been used to decrease the model size.

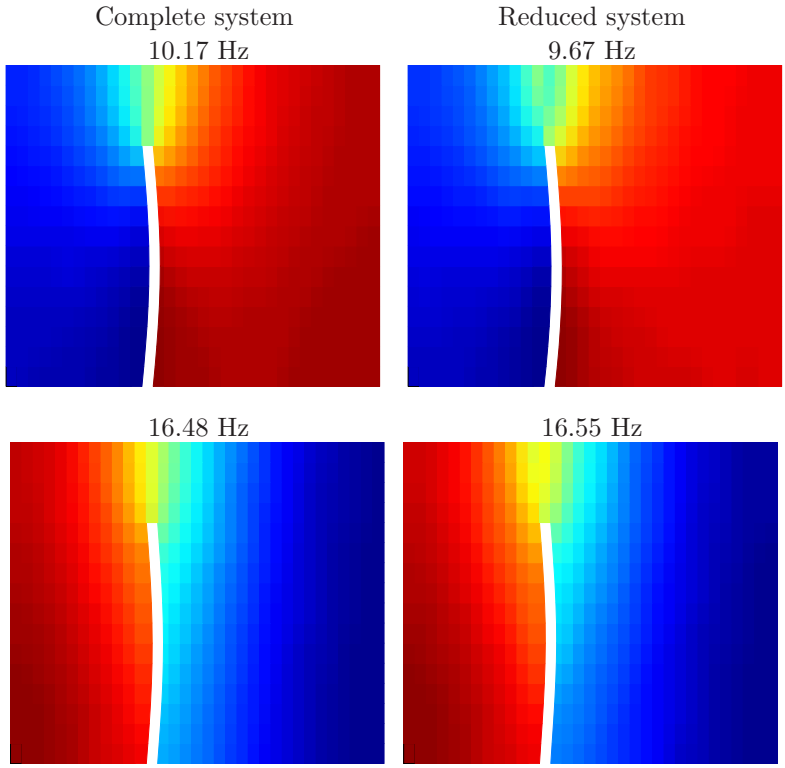

Figure 1.1: *Mode shapes for a enclosed cavity with a flexible wall. The smaller part of the cavity is 3 by 4 meters and the larger part is 5 by four meters. The first two modes for the full system are shown to the left and those for a reduced system to the right.*

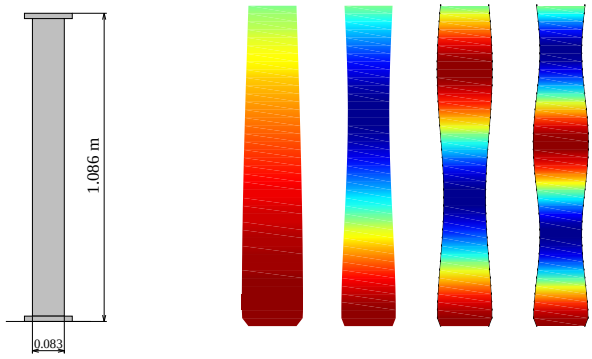

Figure 1.2: *Straight copper pipe filled with water, having a length of 1.083 m, a diameter of 83 mm and a pipe-wall thickness of 3 mm.(left) The first four eigenmodes of the pipe are shown.(right)*

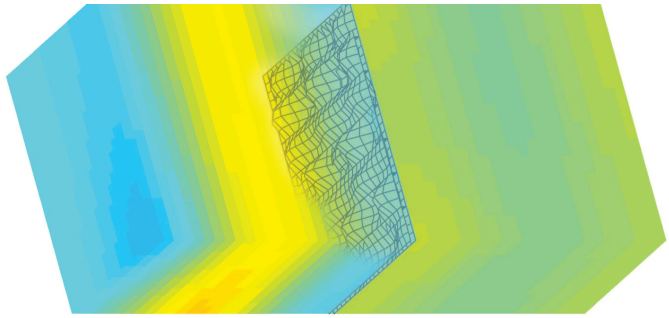

Figure 1.3: *Building acoustics: The acoustic behaviour of double leaf walls is studied in the low frequency range. The figure shows the frequency response to a point source in the room-wall-room system simulating the measurement setup used for determining the sound reduction index of the wall.*

1.4 The development of this thesis

The common denominator in the included articles is that the equations of interest are the coupled structure-acoustic equations and that these equations are solved using the finite element method. The comprising articles treat a wide spectra of applications, but all have these basic equations as a common base. In paper 1 the possibility of a new way of constructing diagonal mass matrices is discussed. This is an important aspect of time-stepping schemes when solving dynamic problems. It is also important in the solution procedures presented in paper 2 and paper 3. In a thesis by Carlsson [18], he also pointed out that in some of the formulations of the fluid-structure systems he studied, a diagonal mass matrix could be very beneficial and that a numerical study of such matrices would be of interest.

In paper 2 a new domain decomposition method for structure-acoustic systems is presented. This paper together with paper 3 deals with a new solution strategy for coupled problems. Both aim at developing new theories for coupled structure-acoustic equations. In paper 4 fluid filled pipes are studied. The industrial application of these pipes could be in submarines but also in nuclear power plants and chemical industries. Again the basic equations are the coupled structure-acoustic equations. The last two papers both deal with room acoustical applications in the low frequency range. In paper 5 a parametric study of double-leaf walls is conducted. In paper 6 the ideas from paper 5 are developed further and ideas how these could be used in the industrial building process are presented. To summarize this, paper 1, 2 and 3 deal with theory development, whereas paper 4, 5 and 6 deal with different industrial applications.

In paper 1, 3 and 4 the author of this thesis carried out both the planning and writing of the papers as well as the numerical implementations and calculations. In paper 2 the own contribution was the numerical implementation and calculations and together with the coauthors the writing of the article. In paper 5 the contribution was on the numerical implementation and in the discussions of the writing of the paper. In the paper 6 all numerical implementations and calculations were carried out by the author. The writing of this paper was also done by the author of the thesis.

Chapter 2

Structure-acoustic analysis

This chapter investigates the analysis of structure-acoustic systems, here limited to systems consisting of a flexible structure in contact with an enclosed acoustic cavity, within the finite element environment. A short literature review is presented here which focuses on the need for this type of analysis and where different formulations in the finite element analysis are discussed. In the sections following, the governing equations of the structure-acoustic problem are given and the finite element formulation of this problem is derived.

2.1 Literature review

The field of structure-acoustic interaction is a thoroughly investigated field of research, see for example Cremer et al. [1], and Fahy [2]). In [3, 4, 5, 6, 7, 8, 9], the structure-acoustic problem is studied using analytical expressions for the two domains. It is evident that the two connecting domains, the flexible structure and the enclosed acoustic cavity, can be strongly coupled and in that case the structure-acoustic system must be studied in a coupled system to evaluate the natural frequencies and the response to dynamic excitation.

The systems often have complex shapes, making analytical solution procedures impossible to use. Numerical methods must be employed. A review of different solution strategies for structure-acoustic problems is given by Atalla [10]. He discusses booth analytical methods and two numerical approaches, namely the finite element method and the boundary element method. The development of structure-acoustic analysis using the finite element method for the study of vehicle interior noise is reviewed by Nefske et al. [11]. A basic introduction to the finite element method is given in, Ottosen and Petersson [12]. A more thorough investigation of the finite element method is found in, for example, the cited works of Bathe [13] or Zienkiewicz and Taylor [14], while a focus on dynamic problems is provided in Clough [15] or Chopra [16].

The formulation of coupled structure-acoustic problems using the finite element method is described, for example, in [17, 18, 19, 20]. The size of the system of equations describing the motion is equal to the number of equations describing the motion. An important property is the sparsity of the system matrices, i.e. only a few positions in these matrices are populated. This property results in that the time for solving the

system of equations is much shorter, compared to solving a fully populated system of equations with equal size.

The primary variable in the structural domain is displacement. For the fluid domain, several different primary variables can be used to describe the motion. The most obvious choice is acoustic pressure, since the acoustic wave equation often is formulated with pressure as primary variable. This leads to the most compact system of equations possible. However, the coupled system of equations is unsymmetric. The pressure formulation was used in [21, 22] to determine normal modes and eigenvalues of complex shaped rigid-wall enclosures and also in [23] to study the transient response of structure-acoustic systems. A two-field formulation, with structural displacements and fluid potential function is achieved with only one degree of freedom per fluid node. The derived system of equations using pressure or displacement potential yields an unsymmetric system of equations. A fluid velocity potential can also be used, where a matrix proportional to velocity is introduced [24]. This system is symmetric, but to achieve that a term that corresponds to a damping matrix has been introduced. To solve the structure-acoustic eigenvalue problem using the two field formulation, one needs an eigenvalue solver that either can handle unsymmetric matrices or can solve quadratic eigenvalue problems. Solving these problems are more computational intensive compared to solving the generalised eigenvalue problem for symmetric systems [25].

In order to achieve a symmetric system of equations describing the structure-acoustic system, a three field formulation with structural displacement, fluid pressure and fluid displacement potential can be used [26, 27]. By condensation of one of the fluid potentials, a symmetric two field system of equations can be achieved [18]. However, the system matrices then lose the positive property of being sparse.

Another possibility is to describe both the structural and fluid domains with displacement as variable. That means that the domains can be described with the same type of solid elements. The fluid domain has no shear stiffness and normal modes with pure rotational motion are introduced. All rotational modes should have the eigenvalue equal to zero. However, spurious non-zero, and thereby non-physical, modes are introduced when using full integration of the solid element. Reduced integration can be used to make all eigenvalues of rotational modes equal to zero [28]; however, due to the reduced integration, the hourglass modes can interact with the correct modes, thereby giving spurious modes with the same frequencies as the correct ones. In [29], the element mass matrix was modified to account for this and the eigenvalue of all spurious modes becomes zero. A mixed displacement based finite element formulation was presented by Bathe [13], also removing the spurious modes.

Different types of methods for model reduction are often employed in structure-acoustic analysis. The most commonly used method is to reduce the system using the normal modes for the structural and fluid domains, derived in separate eigenvalue analysis of the two subdomains [30, 31]. In a paper by Sandberg [32], the un-symmetric eigenvalue problem, achieved when using the structural displacement and fluid pressure as primary variables, is made symmetric using the subdomain modes and matrix scaling. Reduction methods using component mode synthesis were also proposed in, for example, [33, 34]. In the thesis by Carlsson [18], the Lanczos procedure was used in investigating structure-acoustic problems.

2.2 Governing equations and finite element formulation

For the structure-acoustic system, the structure is described by the differential equation of motion for a continuum body assuming small deformations and the fluid by the acoustic wave equation. Coupling conditions at the boundary between the structural and fluid domains ensure the continuity in displacement and pressure between the domains. The governing equations and boundary conditions was described in detail by Carlsson [18]. The variables and material parameters are defined in the following sections, where also the finite element formulation of this coupled problem is derived.

The structure-acoustic problem schematically sketched in figure 2.1. It consists of a fluid domain, Ω_f, and a structure domain, Ω_s. The boundary between the fluid domain and the structure domain is denoted, $\partial\Omega_{sf}$, the fluid boundaries with prescribed pressure, Ω_p, with prescribed velocity, Ω_v, and with a prescribed impedance, Ω_z.

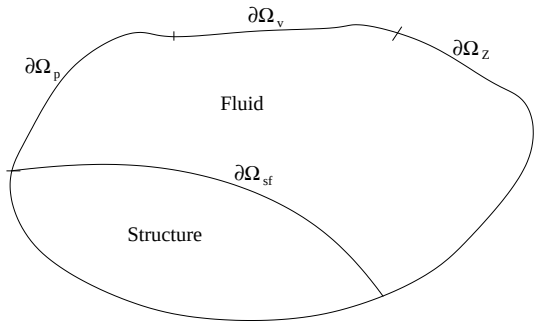

Figure 2.1: *Linear elastic structure filled with a compressible fluid.*

2.2.1 Acoustic fluid domain

The governing equations for an acoustic fluid are derived using the following assumptions for the compressible fluid [18]:

- The fluid is inviscid.
- The fluid only undergoes small translations.
- The fluid is irrotational.

These assumptions lead to the nonhomogeneous wave equation in a bounded fluid domain Ω_f and enclosed by a boundary surface $\partial\Omega_f$.

$$\frac{\partial^2 p}{\partial t}^2 - c_0^2 \boldsymbol{\nabla}^2 p = c_0^2 \frac{\partial q}{\partial t} \tag{2.1}$$

Here $p(t)$ is the dynamic pressure, $q(t)$ is the added fluid mass per unit volume and c_0 is the speed of sound. $\boldsymbol{\nabla}$ denotes a gradient of a variable.

In order to define the pressure field in the fluid domain Ω_f, one boundary condition must be specified at each position on the closed boundary surface $\partial\Omega_f$:

$$\text{imposed pressure} \quad p = \bar{p} \quad \text{on } \partial\Omega_p \tag{2.2}$$

$$\text{imposed normal velocity} \quad v_n = \bar{v}_n \quad \text{on } \partial\Omega_v \tag{2.3}$$

$$\text{imposed normal impedance} \quad p = \bar{Z} v_n \quad \text{on } \partial\Omega_Z \tag{2.4}$$

The finite element formulation of equation (2.1) is derived by multiplying with a test function, v, and integrating over the volume Ω_f.

$$\int_{\Omega_f} v \left(\frac{\partial^2 p}{\partial t}^2 - c_0^2 \boldsymbol{\nabla}^2 p - c_0^2 \frac{\partial q}{\partial t} \right) dV = 0 \tag{2.5}$$

and with Green's theorem the following weak formulation is achieved

$$\int_{\Omega_f} v \frac{\partial^2 p}{\partial t}^2 dV + c_0^2 \int_{\Omega_f} \boldsymbol{\nabla} v \boldsymbol{\nabla} p dV = c_0^2 \int_{\partial\Omega_f} v \boldsymbol{\nabla} p \mathbf{n}_f dS + c_0^2 \int_{\Omega_f} v \frac{\partial q}{\partial t} dV \tag{2.6}$$

where the boundary normal vector $\mathbf{n}_f$ points outwards from the fluid domain. The finite element method approximates the pressure field according to

$$p = \mathbf{N}_f \mathbf{p} \tag{2.7}$$

where $\mathbf{p}$ contains the nodal pressures, and $\mathbf{N}_f$ contains the finite element shape functions for the fluid domain. According to Galerkin the weight functions is then chosen to be the same as the shape functions, i.e.

$$v = \mathbf{N}_f \mathbf{c} \tag{2.8}$$

where $\mathbf{c}$ is the nodal weights and $\mathbf{N}_f$ contains the finite element shape functions for the fluid domain. Inserting this into equation (2.6) and noting that $\mathbf{c}$ is arbitrary gives

$$\begin{aligned} &\int_{\Omega_f} \mathbf{N}_f^T \mathbf{N}_f dV \ddot{\mathbf{p}} + c_0^2 \int_{\Omega_f} (\boldsymbol{\nabla} \mathbf{N}_f)^T \boldsymbol{\nabla} \mathbf{N}_f dV \mathbf{p} = \\ &= c_0^2 \int_{\partial\Omega_f} \mathbf{N}_f^T \boldsymbol{\nabla} p \mathbf{n}_f dS + c_0^2 \int_{\Omega_f} \mathbf{N}_f^T \frac{\partial q}{\partial t} dV \end{aligned} \tag{2.9}$$

The system of equations for an acoustic fluid domain can then be written as

$$\mathbf{M}_f \ddot{\mathbf{p}} + \mathbf{K}_f \mathbf{p} = \mathbf{f}_s + \mathbf{f}_q \tag{2.10}$$

where

$$\begin{aligned} \mathbf{M}_f &= \int_{\Omega_f} \mathbf{N}_f^T \mathbf{N}_f dV \\ \mathbf{K}_f &= c_0^2 \int_{\Omega_f} (\boldsymbol{\nabla} \mathbf{N}_f)^T \boldsymbol{\nabla} \mathbf{N}_f dV \\ \mathbf{f}_s &= c_0^2 \int_{\partial\Omega_f} \mathbf{N}_f^T \boldsymbol{\nabla} p \mathbf{n}_f dS \\ \mathbf{f}_q &= c_0^2 \int_{\Omega_f} \mathbf{N}_f^T \frac{\partial q}{\partial t} dV \end{aligned} \tag{2.11}$$

2.2.2 Boundary terms

The second term on the right hand side in equation (2.10) is the excitation vector due to an external acoustic source. If this acoustic source is a point source of strength $\bar{q}$ located at node i, the source distribution q is

$$q = \bar{q}\delta_i(x_i, y_i, z_i) \tag{2.12}$$

where δ is the Dirac delta function at node i.

The first term on the right hand side in equation (2.10) depends on the boundary conditions. The integration over the boundary surface $\partial\Omega$ can be seen as a sum of the integrations over the subsurfaces $\partial\Omega_p$, $\partial\Omega_v$ and $\partial\Omega_Z$

The boundary with imposed normal velocity will lead to the following term

$$\mathbf{f}_v = c_0^2 \int_{\partial\Omega_v} \rho \mathbf{N}_f \bar{v} dS \tag{2.13}$$

The boundary with the impedance condition leads to a matrix expression, actually a damping matrix

$$\mathbf{C}_f = \int_{\partial\Omega_Z} \rho \bar{A} \mathbf{N}_f^T \mathbf{N}_f dS \tag{2.14}$$

This term is an analogy the case of a beam an elastic foundation that also leads to a contribution on the left hand side of the matrix equation. Equation (2.10) becomes

$$\mathbf{M}_f \ddot{\mathbf{p}} + \mathbf{C}_f \dot{\mathbf{p}} + \mathbf{K}_f \mathbf{p} = \mathbf{f}_s + \mathbf{f}_q \tag{2.15}$$

2.2.3 Structural domain

The structure is described by the equation of motion for a continuum body. The finite element formulation is derived with the assumption of small displacements.

The equation of motion can be written as

$$(\tilde{\boldsymbol{\nabla}}^T \boldsymbol{\sigma} - \rho_S \frac{\partial^2 \mathbf{u}_s}{\partial t^2} + \mathbf{b}) dV = 0 \tag{2.16}$$

To arrive at the finite element formulation for the structural domain, the weak form of the differential equation is derived. This can be done by multiplying equation (2.17) with a weight function, $\mathbf{v} = [v_1\ v_2\ v_3]^T$, and integrating over the structural domain, Ω,

$$\int_{\Omega_s} \mathbf{v}^T (\tilde{\boldsymbol{\nabla}}^T \boldsymbol{\sigma} - \rho_S \frac{\partial^2 \mathbf{u}_s}{\partial t^2} + \mathbf{b}) dV = 0 \tag{2.17}$$

Using Green-Gauss theorem on the first term in equation (2.17) gives

$$\int_{\Omega_s} \mathbf{v}^T \boldsymbol{\nabla}^T \boldsymbol{\sigma} dV = \int_{\partial\Omega_s} (\mathbf{v})^T \mathbf{t} dS - \int_{\Omega_s} (\tilde{\boldsymbol{\nabla}} \mathbf{v})^T \boldsymbol{\sigma} dV \tag{2.18}$$

The surface traction vector $\mathbf{t}$ is related to the Cauchy stress tensor, $\mathbf{S}$, by

$$\mathbf{t} = \mathbf{S}\mathbf{n}_s \tag{2.19}$$

where $\mathbf{n}_s$ is the boundary normal vector pointing outwards from the structural domain and the Cauchy stress tensor is defined by

$$\mathbf{S} = \begin{bmatrix} \sigma_{11} & \sigma_{12} & \sigma_{13} \\ & \sigma_{22} & \sigma_{23} \\ sym. & & \sigma_{33} \end{bmatrix} \tag{2.20}$$

In matrix notations the stresses can be written

$$\boldsymbol{\sigma} = \begin{bmatrix} \sigma_{11} \\ \sigma_{22} \\ \sigma_{33} \\ \sigma_{12} \\ \sigma_{13} \\ \sigma_{23} \end{bmatrix} \tag{2.21}$$

.

The weak form of the problem can then be written

$$\int_{\Omega_s} \mathbf{v}^T \rho_s \frac{\partial^2 \mathbf{u}_s}{\partial t^2} dV + \int_{\Omega_s} (\tilde{\boldsymbol{\nabla}} \mathbf{v})^T \boldsymbol{\sigma} dV - \int_{\partial\Omega_s} (\mathbf{v})^T \mathbf{t} dS - \int_{\Omega_s} \mathbf{v}^T \mathbf{b} dV = 0 \tag{2.22}$$

The finite element approximations of the displacements, $\mathbf{d}$, is introduced by

$$\mathbf{u}_s = \mathbf{N}_s \mathbf{d} \tag{2.23}$$

where $\mathbf{N}_s$ contains the finite element shape functions for the structural domain. The relations between the displacements and strains, can be written

$$\boldsymbol{\varepsilon} = \tilde{\nabla} \mathbf{u}_s \tag{2.24}$$

For an isotropic material, the stresses and strains are related by the constitutive matrix $\mathbf{D}$ given by

$$\boldsymbol{\sigma} = \mathbf{D}\boldsymbol{\varepsilon} \tag{2.25}$$

where

$$\mathbf{D} = \begin{bmatrix} \lambda + 2\mu & \lambda & \lambda & 0 & 0 & 0 \\ \lambda & \lambda + 2\mu & \lambda & 0 & 0 & 0 \\ \lambda & \lambda & \lambda + 2\mu & 0 & 0 & 0 \\ 0 & 0 & 0 & \mu & 0 & 0 \\ 0 & 0 & 0 & 0 & \mu & 0 \\ 0 & 0 & 0 & 0 & 0 & \mu \end{bmatrix} \tag{2.26}$$

The Lamé coefficients, λ and μ, are expressed in the modulus of elasticity, E, the shear modulus, G, and Poisson's ratio, ν by

$$\lambda = \frac{\nu E}{(1+\nu)(1-2\nu)} \tag{2.27}$$

$$\mu = G = \frac{E}{2(1+\nu)} \tag{2.28}$$

Using these relations, the strains can be expressed as

$$\boldsymbol{\varepsilon} = \tilde{\boldsymbol{\nabla}}\mathbf{N}_s\mathbf{d} \tag{2.29}$$

The weight functions are choosen according to Galerkin

$$\mathbf{v} = \mathbf{N}_s\mathbf{c} \tag{2.30}$$

This gives the finite element formulation for the structural domain, when described as a continuum body

$$\int_{\Omega_s} \mathbf{N}_s^T \rho_s \mathbf{N} dV \ddot{\mathbf{d}} + \int_{\Omega_s} (\tilde{\boldsymbol{\nabla}}\mathbf{N}_s)^T \mathbf{D} \tilde{\boldsymbol{\nabla}}\mathbf{N}_s dV \mathbf{d} = \int_{\partial\Omega_s} \mathbf{N}_s^T \mathbf{t} dS + \int_{\Omega_s} \mathbf{N}_s^T \mathbf{b} dV \tag{2.31}$$

and the governing system of equations can be written

$$\mathbf{M}_s\ddot{\mathbf{d}} + \mathbf{K}_s\mathbf{d} = \mathbf{f}_f + \mathbf{f}_b \tag{2.32}$$

where

$$\begin{aligned}
\mathbf{M}_s &= \int_{\Omega_s} \mathbf{N}_s^T \rho_s \mathbf{N}_s dV \\
\mathbf{K}_s &= \int_{\Omega_s} (\tilde{\boldsymbol{\nabla}}\mathbf{N}_s)^T \mathbf{D} \tilde{\boldsymbol{\nabla}}\mathbf{N}_s dV \\
\mathbf{f}_f &= \int_{\partial\Omega_s} \mathbf{N}_s^T \mathbf{t} dS \\
\mathbf{f}_b &= \int_{\Omega_s} \mathbf{N}_s^T \mathbf{b} dV
\end{aligned} \tag{2.33}$$

2.2.4 The coupled structure-acoustic system

The dynamic coupling of the different domains, structure and fluid, is fulfilled by assuming continuity of the fluid displacements and structural displacements in the normal direction to the interface. Introducing the normal vector $\mathbf{n} = \mathbf{n}_f = -\mathbf{n}_s$, the displacement boundary condition can be written

$$\mathbf{u}_s\mathbf{n}_s|_{\partial\Omega_{sf}} = \mathbf{u}_f\mathbf{n}_f|_{\partial\Omega_{sf}} \tag{2.34}$$

and the continuity in pressure

$$\sigma|_n = -p \tag{2.35}$$

where p is the acoustic fluid pressure. The structural stress tensor at the boundary $\partial\Omega_{sf}$ thus becomes

$$\mathbf{S} = -p \begin{bmatrix} 1 & 0 & 0 \\ 0 & 1 & 0 \\ 0 & 0 & 1 \end{bmatrix} \tag{2.36}$$

and the structural force term providing the coupling to the fluid domain, $\mathbf{f}_f$ (in equation (2.32)), can be written

$$\mathbf{f}_f = \int_{\partial\Omega_{sf}} \mathbf{N}_s^T(-p) \begin{bmatrix} 1 & 0 & 0 \\ 0 & 1 & 0 \\ 0 & 0 & 1 \end{bmatrix} \mathbf{n}_s dS = \int_{\partial\Omega_{sf}} \mathbf{N}_s^T \mathbf{n} p dS = \int_{\partial\Omega_{sf}} \mathbf{N}_s^T \mathbf{n}\mathbf{N}_f dS \mathbf{p} \tag{2.37}$$

Note that the structural boundary normal vector $\mathbf{n}_s$ is replaced with the normal vector $\mathbf{n}$ pointing in the opposite direction. The force acting on the structure is expressed in the acoustic fluid pressure.

For the fluid partition the coupling is introduced in the force term $\mathbf{f}_S$ (in equation (2.10)). Using the relation between pressure and acceleration in the fluid domain

$$\boldsymbol{\nabla} p = -\rho_0 \frac{\partial^2 \mathbf{u}_f(t)}{\partial t^2} \tag{2.38}$$

and the boundary condition in equation (2.34), the force acting on the fluid can be described in terms of structural acceleration

$$\mathbf{n}^T \boldsymbol{\nabla} p|_{\partial\Omega_{sf}} = -\rho_0 \mathbf{n}^T \frac{\partial^2 \mathbf{u}_f}{\partial t^2}|_{\partial\Omega_{sf}} = -\rho_0 \mathbf{n}^T \frac{\partial^2 \mathbf{u}_s}{\partial t^2}|_{\partial\Omega_{sf}} = -\rho_0 \mathbf{n}^T \mathbf{N}_s \ddot{\mathbf{d}}|_{\partial\Omega_{sf}} \tag{2.39}$$

and the boundary force term of the acoustic fluid domain, $\mathbf{f}_S$, can be expressed in structural acceleration

$$\mathbf{f}_s = -c_0^2 \int_{\partial\Omega_{fs}} \mathbf{N}_f^T \mathbf{n}^T \boldsymbol{\nabla} p dS = -\rho_0 c_0^2 \int_{\partial\Omega_{fs}} \mathbf{N}_f^T \mathbf{n}^T \mathbf{N}_s dS \ddot{\mathbf{d}} \tag{2.40}$$

The introduction of a spatial coupling matrix

$$\mathbf{H}_{sf} = \int_{\partial\Omega_{sf}} \mathbf{N}_s^T \mathbf{n} \mathbf{N}_f dS \tag{2.41}$$

allows the coupling forces to be written as

$$\mathbf{f}_f = \mathbf{H}_{sf} \mathbf{p} \tag{2.42}$$

and

$$\mathbf{f}_s = -\rho_0 c_0^2 \mathbf{H}_{sf}^T \ddot{\mathbf{d}} \tag{2.43}$$

The structure-acoustic problem can then be described by an unsymmetrical system of equations

$$\begin{bmatrix} \mathbf{M}_s & \mathbf{0} \\ \rho_0 c_0^2 \mathbf{H}_{sf}^T & \mathbf{M}_f \end{bmatrix} \begin{bmatrix} \ddot{\mathbf{d}} \\ \ddot{\mathbf{p}} \end{bmatrix} + \begin{bmatrix} \mathbf{K}_s & -\mathbf{H}_{sf} \\ 0 & \mathbf{K}_f \end{bmatrix} \begin{bmatrix} \mathbf{d} \\ \mathbf{p} \end{bmatrix} = \begin{bmatrix} \mathbf{f}_b \\ \mathbf{f}_q \end{bmatrix} \tag{2.44}$$

This system is studied through out this thesis.

2.3 Mass lumping

2.3.1 Introduction.

Mass matrices used within the finite element method can be derived in many different ways. In the early days of the finite element method it was common to just place particle masses, m_i, at nodes i of an element such that $\sum m_i$ became the total element mass. Particle 'lumps' had no rotary inertia unless rotary inertia was arbitrarily assigned, as sometimes was done for the rotation degrees of freedom of beams and plates. This method of generating mass matrices, called *ad hoc lumping*, is probably the most intuitive lumping method. More sophisticated lumping methods have been developed since then.

One of the advantages of lumped mass matrices is that they are diagonal. This property could be utilized in many situations, e.g. in fluid structure interaction problems where in some formulations the mass matrix has to be inverted. There are also some time stepping schemes for solving dynamic problems, where a diagonal mass matrix is very beneficial, e.g. in the central difference method.

In this chapter the different methods to calculate mass matrices are described , e.g. lumping by nodal quadrature, row-sum technique, special lumping technique, consistent diagonal and lumping by minimization of modal errors. Later mixed matrices are discussed, i.e. combinations between lumped and consistent mass matrices, and finally frequency dependent mass matrices are described. Both of these methods create full matrices.

2.3.2 Consistent and non-consistent mass matrices.

The consistent mass matrix is based on the same shape functions as the stiffness matrix

$$\mathbf{M}_c = \int_\Omega \mathbf{N}^T \rho \mathbf{N} dV \tag{2.45}$$

The lumping procedure of a mass matrix can be seen when the standard shape functions, $\mathbf{N}_i$, are substituted by piecewise linear functions, $\bar{\mathbf{N}}_i$ and Eq. (2.45) is replaced by

$$\mathbf{M}_l = \int_\Omega \bar{\mathbf{N}}^T \rho \bar{\mathbf{N}} dV \tag{2.46}$$

in which $\bar{N}_i$ are non-overlapping functions covering the whole element. It is the fact that the functions are non-overlapping that makes the matrix in Eq. (2.46) diagonal. There are infinite possibilities to chose such an approximation. For convergence, it can be shown that only three conditions must be satisfied

$$\begin{array}{rcll} \bar{N}_i & = & 1 & \text{at } x_i \\ \bar{N}_i & = & 0 & \text{at } x_j \\ \sum \bar{N}_i & = & 1 & \end{array} \tag{2.47}$$

Example of shape functions can be seen in Figures 2.2 and 2.3.

The non-consistent mass matrices could be divided into diagonal mass matrices and "mixed mass matrices". The latter are combinations of the consistent mass matrix and a lumped mass matrix and therefore not diagonal, but often yields more accurate solution than consistent mass matrices.

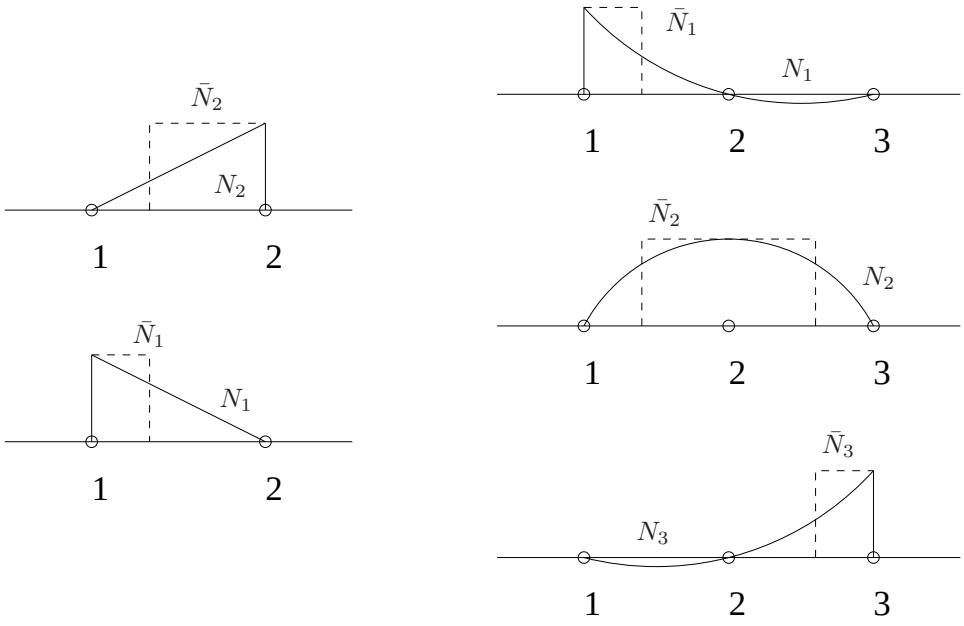

Figure 2.2: *Shape functions for linear and parabolic elements.*

2.3.3 Mass lumping by nodal quadrature

The idea of nodal quadrature is to use the nodes as integration points in the numerical integration formula. Normally we would have used Gauss points according to Gauss integration rules, and because more than one shape function in an element has a non-zero value at the gauss points, off-diagonal terms are generated. The formula for the mass matrix at element level is

$$\begin{aligned} m_{ij}^e &= \delta_{ij} \int N_a \rho N_b \, d\Omega \\ &\cong \delta_{ij} \sum_{c=1}^{n_{eq}} N_a(\xi_c) \rho N_b(\xi_c) J(\xi_c) W_c \\ &= \begin{cases} \delta_{ij} \rho J(\xi_a) W_a & a = b \\ 0 & a \neq b \end{cases} \end{aligned} \tag{2.48}$$

where $J(\xi_a)$ is the Jacobian evaluated in the points ξ_a, i.e. in the nodes, and W_a is the weight function for each integration point. In short, this formula means that the mass matrix is evaluated with the same numerical procedure, only the integration points are chosen to coincide with the nodes, and this choice makes the off-diagonal terms vanish. A theory of nodal quadrature is presented in [35] which describes under what conditions the nodal quadrature mass matrix is convergent and retains full order of accuracy. If p is the highest degree of the shape function N_i, and m is the highest order of derivative in the strain energy expression, then the mass matrices lumped with the quadrature rule

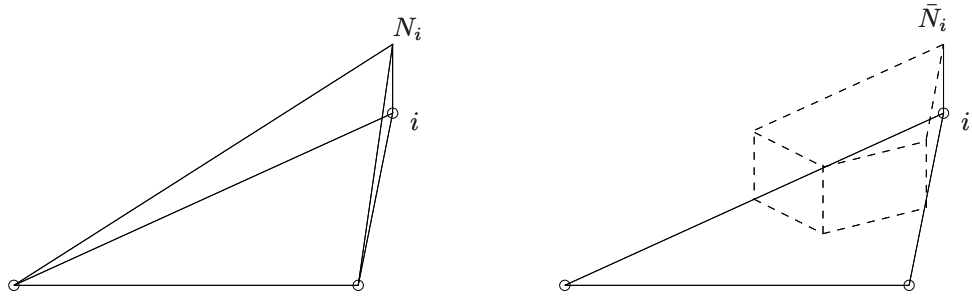

Figure 2.3: *Linear and piecewise constant shape functions for a triangle.*

with degree of at least $2(k-m)$ will yield comparable accuracy and convergence with the consistent mass matrix. Mass matrices lumped this way are often called *"optimally lumped"*. The method has, however, some drawbacks. For some element types, e.g. the two-dimensional eight node quadrilateral, the method produces negative entries in the lumped matrix. This can't be handled by standard eigenvalue solvers, and could also cause some non-physical behavior. Another problem could occur when trying to lump axisymmetric elements. In that case one obtains zero masses along the axis of symmetry. This is also a problem for eigenvalue solvers, because the mass matrix becomes indefinite. A third problem is elements with rotational degrees of freedom, e.g. beam elements. When nodal quadrature is used on these elements, one obtains block-diagonal matrices, which are of less importance here.

2.3.4 Row-sum technique

As the name row-sum technique implies, the entries in each row are summed and lumped on the diagonal. This can be formulated as

$$m_{ij}^e = \begin{cases} \delta_{ij} \int_{\Omega^e} \rho N_a \, d\Omega & a = b \\ 0 & a \neq b \end{cases} \tag{2.49}$$

One drawback of the method is that it produces negative masses for some elements, e.g. the two-dimensional eight node quadrilateral.

2.3.5 Special lumping technique

The idea behind this method is to use only the diagonal terms of the consistent mass matrix, but to scale them in such a way that the total mass of the element is preserved. The method was developed by Hinton, Rock and Zienkiewicz [36], and is therefore often called the 'HRZ scheme'. One advantage of the method is that it always produces positive definite lumped mass matrices. The formula is

$$m_{ij}^e = \begin{cases} \alpha \delta_{ij} \int_{\Omega^e} \rho N_a^2 \, d\Omega & a = b \\ 0 & a \neq b \end{cases} \tag{2.50}$$

where

$$\alpha = \frac{\int_{\Omega^e} \rho \, d\Omega}{\sum_{a=1}^{n_{en}} \int_{\Omega^e} \rho N_a^2 \, d\Omega} = \frac{\text{total element mass}}{\begin{array}{l}\text{sum of diagonal entries associated} \\ \text{with one translational degree of} \\ \text{freedom}\end{array}} \tag{2.51}$$

Note that all diagonal entries from the consistent mass matrix are scaled in the same way, including entries that are asociated with rotaitonal degrees of freedom. The special lumping technique is the only method that works on arbitrary elements, and even though no mathemtical theory of the method has been presented it is a very robust method.

2.3.6 Consistent diagonal mass matrix

Another possibility is described by Sauer [37], who has developed consistent diagonal mass matrices for the four-node quadrilateral and the eight-node hexadron elements. The idea behind this method is to add a contribution to the standard shape functions which make the off-diagonal entries vanish in the mass matrix. For the four-node element the shape functions look like

$$\begin{aligned} N_1 &= 0.25\left[1-(1-\alpha)\xi-\alpha\xi^3\right]\left[1-(1-\alpha)\eta-\alpha\eta^3\right] \\ N_2 &= 0.25\left[1+(1-\alpha)\xi+\alpha\xi^3\right]\left[1-(1-\alpha)\eta-\alpha\eta^3\right] \\ N_3 &= 0.25\left[1+(1-\alpha)\xi+\alpha\xi^3\right]\left[1+(1-\alpha)\eta+\alpha\eta^3\right] \\ N_4 &= 0.25\left[1-(1-\alpha)\xi-\alpha\xi^3\right]\left[1+(1-\alpha)\eta+\alpha\eta^3\right] \end{aligned} \tag{2.52}$$

The equations above contain a free parameter which has to be determined. The expressions for the off-diagonal terms of the mass matrix are used, and α is selected so that these terms become zero, i.e.

$$\int \rho N_i N_j d\Omega = 0 \qquad i \neq j \tag{2.53}$$

Finding such a value of the parameter α, however, is only possible if one chooses a 2 by 2 integration scheme. In that case one obtains for the four-node element, $\alpha = -1.5(1-\sqrt{3})$. A projection on the x-axis of the element shape functions N_1 and N_2 can be seen in Figure 2.4.

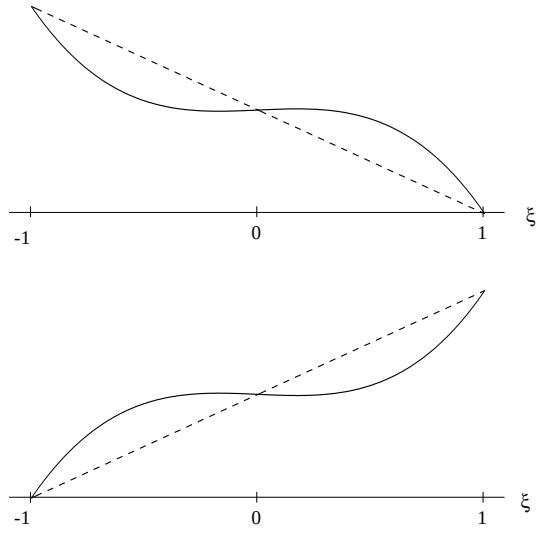

Figure 2.4: *Projection on the ξ-axis of shape functions N_1 (above) and N_2 (below). Dashed line is consistent shape function and solid line is shape function according to Sauer.*

For the eight-node volume element the shape functions are expanded in the same way as for the four-node element.

However, there is one thing to observe. This method gives diagonal mass matrices but it also gives other stiffness matrices than the standard shape functions would have done. In fact, this difference in the stiffness matrices seems to be the major reason why this method gives good results in eigenvalue analyses, see [37].

2.3.7 Mixed mass matrices.

Since consistent mass matrices overestimate the natural frequencies, whereas lumped mass matrices usually underestimate them, a linear combination of the two can yield more satisfactory results. Let

$$M_{mix} = (1-\gamma)M_C + \gamma M_L \tag{2.54}$$

where the formulation for the lumped mass matrix corresponds to $\gamma = 1$ and that for the consistent mass matrix to $\gamma = 0$. All other possible values of γ correspond to a 'mixed matrix'.

This procedure can be seen as combining the shape functions of each element from the consistent and the lumped matrix into a single function, see [38] and [39]. Various mixed shape functions for a linear bar element are shown in Figure 2.5

2.3.8 Freqency dependent mass matrices.

So far, a freqency independent approach to discretize the model has been described. This leads, both in the consistent and non-consistent mass matrix formulations, to the eigenvalue problem

$$(\mathbf{K} - \omega_n^2 \mathbf{M})\mathbf{X}_n = 0 \tag{2.55}$$

In the freqency dependent approach, however, it is assumed that the finite element shape functions depend on the unknown frequency ω. This means that the element shape function could be written

$$\mathbf{N} = (\mathbf{N}_0 + \omega\mathbf{N}_1 + \omega^2\mathbf{N}_2 + ...) \tag{2.56}$$

This results in a quadratic eigenvalue problem

$$[\mathbf{K}_0 - \omega^2\mathbf{M}_0 - \omega^4(\mathbf{M}_2 - \mathbf{K}_4) - ...]\mathbf{X} = 0 \tag{2.57}$$

There are different ways of solving a quadratic eigenvalue problem, but as a general rule it always takes more computational effort to solve such a problem as compared to a standard eigenvalue problem. This disadvantage has to be weighed against the improved accuracy of the eigen frequencies. The method has not been implemented in any commercial finite element program.

To see that a standard eigenvalue problem of a continuous body actually is an approximation of the frequency dependent problem, we can rewrite Eq. (2.55)

$$\left[-\omega^2 \begin{bmatrix} \mathbf{M}_{bb} & \mathbf{M}_{bi} \\ \mathbf{M}_{ib} & \mathbf{M}_{ii} \end{bmatrix} + \begin{bmatrix} \mathbf{K}_{bb} & \mathbf{K}_{bi} \\ \mathbf{K}_{ib} & \mathbf{K}_{ii} \end{bmatrix}\right] \begin{Bmatrix} \mathbf{u}_b \\ \mathbf{u}_i \end{Bmatrix} = \{0\} \tag{2.58}$$

where $\mathbf{u}_b$ are the selected degrees of freedom in the model, and $\mathbf{u}_i$ are the dependent degrees of freedom, which we want to eliminate. If we solve for $\mathbf{u}_i$

$$\mathbf{u}_i = -(-\omega^2\mathbf{M}_{ii} + \mathbf{K}_{ii})^{-1}(-\omega^2\mathbf{M}_{ib} + \mathbf{K}_{ib})\{\mathbf{u}_b\} \tag{2.59}$$

the resulting eigenvalue problem for the chosen degrees of freedom is

$$\left[-\omega^2\mathbf{M}_{bb} + \mathbf{K}_{bb} - (-\omega^2\mathbf{M}_{bi} + \mathbf{K}_{bi})(-\omega^2\mathbf{M}_{ii} + \mathbf{K}_{ii})^{-1}(-\omega^2\mathbf{M}_{ib} + \mathbf{K}_{ib})\right]\{\mathbf{u}_b\} = \{0\} \tag{2.60}$$

which implies an eigenvalue problem of the form

$$\left[\mathbf{A} - \omega^2\mathbf{B} - \omega^4\mathbf{C}...\right]\{\mathbf{u_b}\} = \{0\} \tag{2.61}$$

where $\mathbf{A}$, $\mathbf{B}$ and $\mathbf{C}$ are functions of the original partitioned matrices in 2.58. Since a discretized dynamic problem is a reduced set of the continuous structural formulation, the standard eigenvalue problem is just an approximation of the frequency dependent problem in 2.57

$$[\mathbf{K}_0 - \omega^2\mathbf{M}_0 - \omega^4(\mathbf{M}_2 - \mathbf{K}_4) - ...]\mathbf{X} = 0 \tag{2.62}$$

In the numerical investigation the frequency dependent approach will not be tested.

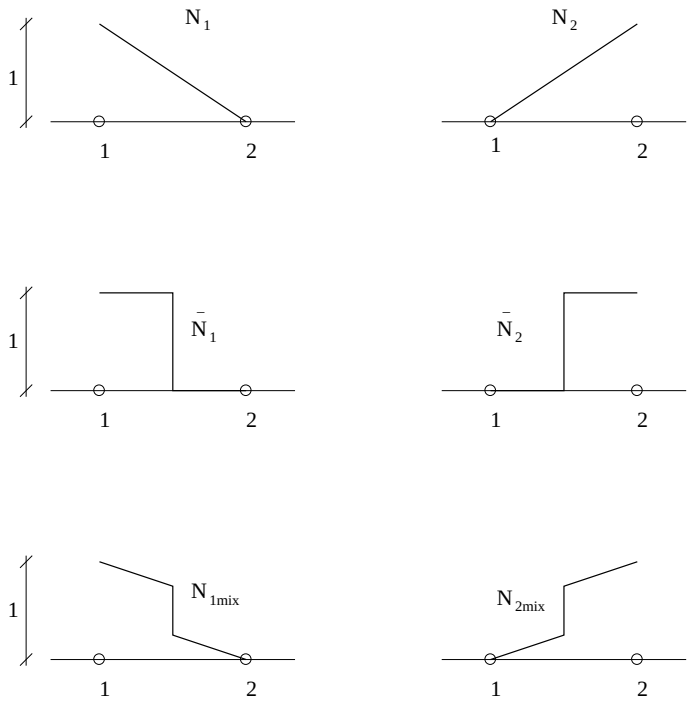

Figure 2.5: *Shape functions for a linear bar element. Above is a consistent element, in the middle a lumped element and below a mixed element.*

2.4 Dynamic analysis of piping systems

2.4.1 Introduction.

Cylindrical pipes are widely used in industrial applications, such as e.g. nuclear plants and pressure industries, and the vibrations that occur in these pipes are of great interest to the designer. The dynamic behaviour includes both transient excitation, e.g. caused by pressure pulses, and steady-state excitation caused by unbalanced rotating machinery, e.g. pumps.

These piping systems can be very large and an analysis of these systems using a three-dimensional model is often very inconvenient. Therefore simplified approaches must be used to analyze these systems. The first thing to decide is whether the analysis should be coupled or not , i.e. if the fluid-structure interaction should be taken into account. An approximate approach would be to perform the analysis in two steps; first the fluid response is calculated assuming that the structure is rigid and then the structural response is calculated due to the calculated fluid pressures. In most cases this approach yield a conservative estimate of the structural response, but there are also cases when a significant resonance between the fluid and the structure occurs and then coupled analysis must be evaluated. In this study a model including the effects of fluid structure interaction will be developed.

When analyzing pipes it is wise to first study vibration patterns for cylindrical shells, seen in Figures 2.6, 2.7 and 2.8.

The vibration corresponding to $n = 0$ in Figure 2.7 is often called the breathing mode. This mode is the dominant mode in cases with fluid transients, i.e pressure pulses, and the coupling between shell and fluid is strong. The next mode in Figure 2.7, $n = 1$, is called the beam-bending mode. As can bee seen from the figure, this mode does not involve any cross-section area change, i.e. no coupling occurs and the contained fluid only acts as an added mass. The beam-bending mode is usually the dominant aspect in low-frequency vibrations in piping systems. The next modes, $n = 2$(ovalization), $n = 3$ etc. are more complex in their forms and will not be studied further in this report. The coupling between fluid and structure in these modes are not as strong as for the breathing mode. In Figure 2.6 the axial mode pattern associated with the radial vibration modes are shown, and in Figure 2.8 the axially vibration pattern corresponding to the beam-bending mode, $n = 1$, in Figure 2.7 are shown.

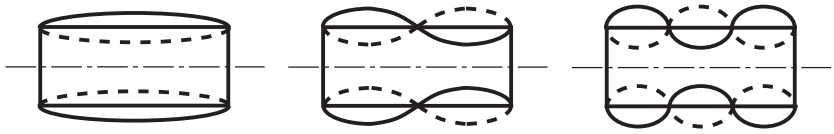

Figure 2.6: *Axial displacement mode shapes of a circular pipe.*

Low-frequency steady-state vibrations.

For low-frequency dynamic excitation of fluid-filled piping systems, the pipes responds only in their beam modes, $n = 1$ and not in lobar modes, see Figures 2.7 and 2.8.

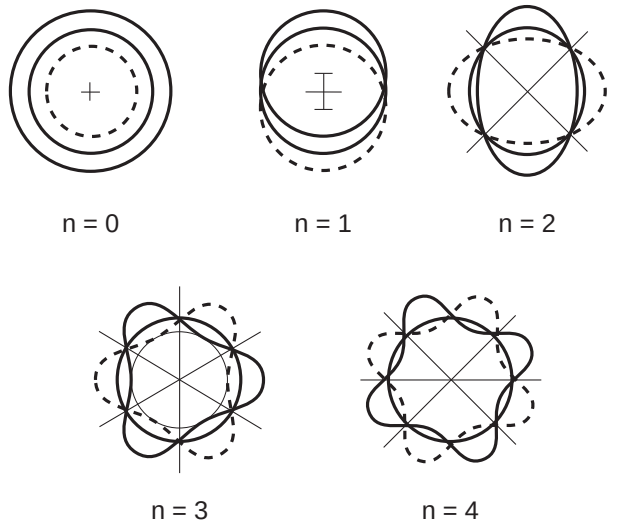

Figure 2.7: *Cross-sectional radial displacement mode shapes of a circular pipe.*

Figure 2.8: *Beam bending mode shapes of a circular pipe.*

Except for the inertial effect the fluid-structure coupling is assumed to occur only at the pipe bends. This means that the finite element model can be built in the following way. Beam elements are used to model both the straight pipe-sections and the elbows. Due to the fact that the pipe bend is more flexible than an equivalent length of a straight pipe either a flexibility factor could be used with the ordinary beam elements or special elbow elements could be used to compensate for the bend effect. The acoustic fluid inside the pipe is usually modeled with one-dimensional acoustic elements. This kind of analyses can be done with a standard finite element program for structural analysis if the material constants for the fluid is adjusted. The fluid elements are modeled with structural rod elements and are assigned the actual mass density ρ for the fluid and the Youngs modulus E is given by

$$E = B/(1 + 2rB/E_s t) \tag{2.63}$$

where B is the fluid bulk modulus, r is the mean radius of the pipe, E_s is the Youngs modulus of the pipe material and t is the pipe wall thickness. The denominator in Eq. 2.63 is a corrective factor which account for the elasticity of the pipe. The reactive pressure from the fluid affects the structure at the pipe bends. The fluid displacements are constrained to move with the corresponding structural points in the transverse direction, meaning that the fluid acts as an added mass to these vibrations. In the axial direction the fluid is free to slide relative to the beam. This model has proven to be valid for frequencies up to about one half of the lowest acoustic eigenfrequency.

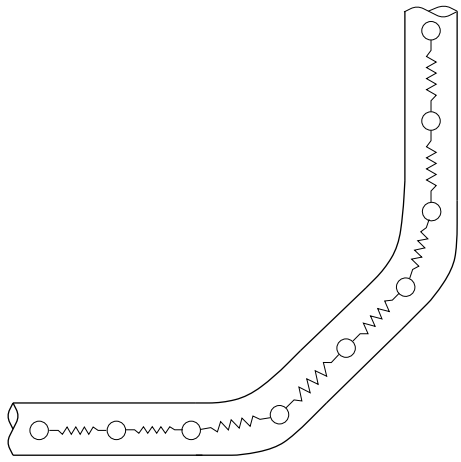

Figure 2.9: *Pipe with acoustic fluid, where the fluid can be seen as spring-connected masses, free to move along the pipe in the axial direction but constrained to move with the pipe in the radial direction.*

2.4.2 Transient analysis of fluid-filled pipes.

The transient response of fluid-filled pipes is usually referred to as waterhammer. Waterhammer involves large transient pressure pulses which may damage the pipe and its components. These pressure pulses are generated by e.g. rapid closing or opening of valves, or by stopping and starting pumps. In conventional waterhammer analyses pipe elasticity is not incorporated in the propagation speed of the pressure waves. This could be acceptable for rigid accord pipes but for less restrained systems the fluid structure interaction may become of importance. This means that a system of coupled equations, one set for the fluid with the pressure as the primary variable and one set for the structure with displacement as the primary variable, has to be solved simultaneously. Three different liquid-pipe coupling mechanisms can be distinguished; friction coupling, Poisson coupling and junction coupling. Friction coupling represents the mutual friction between the liquid and the pipe. This phenomena is not included in the present study. The Poisson coupling relates the pressure in the liquid to the axial stresses in the pipe through the radial contraction or expansion of the pipe wall. It is associated with the breathing, n=0 in Figure 2.7. Whereas friction and Poisson coupling act along the pipe, junction coupling acts at specific points in the piping system such as e.g. bends. When a junction has the possibility to move in the axial pipe direction, which is the direction of the pressure wave, mutual forces between fluid and pipe system may interact, which is known as junction coupling.

A procedure called the method of characteristics, MOC, is often used when solving waterhammer equations where the pressure pulse is of primary interest, but in situations where one is interested in both the pressure wave and the structural behavior of the pipe, it could be convenient to use the finite element method to solve the equations.

The effects of fluid structure interaction are problem dependent, the calculations including fluid structure interaction may or may not lead to higher pressures and stresses.

Chapter 3

Concluding Remarks and Contributions

This introduction was intended to give the reader a short background to the six different papers that comprises this thesis. Both in terms of trying to explain how the articles are connected to each other, and also to give a deeper general background to the field of structure-acoustic analysis and to give a detailed background to two special topics, namely mass lumping and transient analysis of fluid filled pipes.

The overall aim of the work presented in this thesis has been to develop analysis methods and to study engineering applications within the field of structure acoustic analysis. This is a quite general goal, and to be more precise the most important results of the work can be summarised in the following items:

- A new method for mass matrix lumping was developed in paper 1, applicable to many dynamic finite element problems
- In paper 2 a new domain decomposition method was developed for structure acoustic problems.
- In paper 3 a new solution method for a special case of coupled problems was presented.
- In paper 4 a method for a simplified analysis procedure of fluid-filled pipes was discussed.
- In paper 5 and in paper 6 the finite element method was used to study room acoustical problems in the low frequency range. Several examples showed the usability of the method in these papers.

Naturally the field of structure-acoustic analysis is not ready as a research field. There are many things yet to be investigated. Better solution methods, better methods to model materials and damping. Methods that make it possible to conduct the analysis at a higher valid frequency limit. These examples all deal with new methods. But there are also things to be done using existing methods, only using them in a new way, as in paper 6. This paper is only suggestion for a starting point for these procedures, much more work needs to be done in this field.

Bibliography

[1] L. Cremer, M. Heckl, and E. Ungar. *Structure-Borne Sound*. Springer-Verlag, Berlin, 1988.

[2] F. Fahy. *Sound and structural vibration*. Academic Press, London, 1985.

[3] A. J. Pretlove. Free vibrations of a rectangular panel backed by a closed rectangular cavity. *Journal of Sound and Vibration*, 2(3):197–209, 1965.

[4] A. J. Pretlove. Forced vibrations of a rectangular panel backed by a closed rectangular cavity. *Journal of Sound and Vibration.*, 3(3):252–261, 1966.

[5] R. W. Guy. The response of a cavity backed panel to external airborne excitation: A general analysis. *The Journal of the Acoustical Society of America*, 65(3):719–731, 1979.

[6] E. H. Dowell, G. F. Gorman, and D. A. Smith. Acoustoelasticity: General theory, acoustic natural modes and forced response to sinusodal excitation, including comparasons with experiments. *Journal of Sound and Vibration*, 52(4):519–542, 1977.

[7] J. Pan and D. A. Bies. The effect of fluid-structural coupling on sound waves in an enclosure–theoretical part. *The Journal of the Acoustical Society of America*, 87(2):691–707, 1990.

[8] K.L. Hong and J. Kim. Analysis of free vibration of structural-acoustic coupled systems, part i: Development and verification of the procedure. *Journal of Sound and Vibration.*, 188(4):561–575, 1995.

[9] K. L. Hong and J. Kim. Analysis of free vibration of structural-acoustic coupled systems, part ii: Two- and three-dimensional examples. *Journal of Sound and Vibration.*, 188(4):577–600, 1995.

[10] N. Atalla and R. J. Bernhard. Review of numerical solutions for low-frequency structural-acoustic problems. *Applied Acoustics*, 43(2):271–294, 1994.

[11] D. J. Nefske, J. A. Wolf, and L. J. Howell. Structural-acoustic finite element analysis of the automobile compartment: A review of current practice. *Journal of Sound and Vibration*, 80(2):247–266, 1982.

[12] N. Ottosen and H. Peterson. *Introduction to the Finite Element Method*. Prentice Hall, New York, 1992.

[13] K.-J. Bathe. *Finite Element Procedures*. Prentice Hall, New York, 1996.

[14] O. C. Zienkiewicz and R. L.Taylor. *The Finite Element Method*, volume 1 and 2. MacGraw-Hill, London, 1994.

[15] R. Clough and J. Penzien. *Dynamics of Structures*. McGraw-Hill, London, 1993.

[16] A. Chopra. *Dynamics of Structures*. Prentice Hall, New York, 2001.

[17] G. Sandberg. Finite element modelling of fluid-structure interaction. TVSM 1002, Structural Mechanics, LTH, Lund University, Box 118, SE-221 00 Lund, Sweden, 1986.

[18] H. Carlsson. Finite element analysis of structure-acoustic systems; formulations and solution strategies. TVSM 1005, Structural Mechanics, LTH, Lund University, Lund, Sweden, 1992.

[19] H. Morand and R. Ohayon. *Fluid structure interaction*. John Wiley & sons, Chichester, 1995.

[20] G. C. Everstine. Finite element formulations of structural acoustics problems. *Computers & Structures*, 65(2):307–321, 1997.

[21] A. Craggs. The use of three-dimensional acoustic finite elements for determining the natural modes and frequencies of complex shaped enclosures. *Journal of Sound and Vibration*, 23(3):331–339, 1972.

[22] M. Petyt, J. Lea, and G. H. Koopmann. A finite element method for determining the acoustic modes of irregular shaped cavities. *Journal of Sound and Vibration*, 45(4):495–502, 1976.

[23] A. Craggs. The transient response of a coupled plate-acoustic system using plate and acoustic finite elements. *Journal of Sound and Vibration*, 15(4):509–528, 1971.

[24] G. C. Everstine. A symmetric potential formulation for fluid-structure interaction. *Journal of Sound and Vibration*, 71(1):157–160, 1981.

[25] G. H. Golub and C. F. Van Loan. *Matrix Computations*. The Johns Hopkins University Press, Baltimore, 1990.

[26] H. Morand and R. Ohayon. Substructure variational analysis of the vibrations of coupled fluid-structure systems. finite elemtent results. *International Journal of Numerical Methods in Engineering*, 14:741–755, 1979.

[27] G. Sandberg and P. Göransson. A symmetric finite element formulation for acosutic fluid-structure interaction analysis. *Journal of Sound and Vibration*, 123(3):507–515, 1988.

[28] N. Akkas, H. U. Akay, and C. Yilmaz. Applicability of general-purpose finite element programs in solid-fluid interaction problems. *Computers & Structures*, 10:773–783, 1979.

[29] H. C. Chen and R. L. Taylor. Vibration analysis of fluid-solid systems using a finite element displacement formulation. *International Journal of Numerical Methods in Engineering*, 29:683–698, 1990.

[30] J. A. Wolf. Modal synthesis for combined structural-acoustic systems. *AIAA Journal*, 15:743–745, 1977.

[31] R. Ohayon. Reduced symmetric models for modal analysis of internal structural-acoustic and hydroelastic-sloshing systems. *Computer methods in applied mechanics and engineering*, 190:3009–3019, 2001.

[32] G. Sandberg. A new strategy for solving fluid-structure problems. *International Journal of Numerical Methods in Engineering*, 38:357–370, 1995.

[33] W. J. T. Daniel. Modal methods in finite element fluid-structure eigenvalue problems. *International Journal of Numerical Methods in Engineering*, 15:1161–1175, 1980.

[34] J. Wandinger. A symmetric Craig-Bampton method of coupled fluid-structure systems. *Engineering Computation*, 15(4):450–461, 1998.

[35] G. Strang G. and G.J. Fix. *An analysis of the finite element method.* McGraw-Hill, London, 1973.

[36] T. Rock T E. Hinton. A note on mass lumping and related processes in the finite element method. *Earthquake engineering and structural dynamics*, 4:245–249, 1975.

[37] G. Sauer. Consistent diagonal mass matrices for the isoparametric 4-node quadrilateral and 8-node hexadron elements. *Communications in numerical methods in Engineering*, 9:35–43, 1993.

[38] K. Kim. A review of mass matrices for eigenproblem. *Computers and structures*, 46:1041–1049, 1993.

[39] J. Dubois C. Stavrinidis, J. Clinckemaillie. New concepts for finite-element mass matrix formulations. *AIAA Jnl*, 27:1249–1255, 1989.

THE INCLUDED PAPERS

Paper 1

MASS MATRICES BY MINIMIZATION OF MODAL ERRORS

P-A. HANSSON, AND G. SANDBERG

INTERNATIONAL JOURNAL FOR NUMERICAL METHODS IN ENGINEERING, 40, 4259-4271(1997)

INTERNATIONAL JOURNAL FOR NUMERICAL METHODS IN ENGINEERING, VOL. 40, 4259–4271 (1997)

MASS MATRICES BY MINIMIZATION OF MODAL ERRORS

PER-ANDERS HANSSON* AND GÖRAN SANDBERG

Division of Structural Mechanics, Lund Institute of Technology, Lund University, PO Box 118, S-221 00 Lund, Sweden

ABSTRACT

A new approach to constructing mass matrices is presented, based on expressing it through use of a variable parameter. This allows the mass matrix to be adjusted in such a way that a simple eigenvalue problem get the best solution possible in terms of some error measure. This procedure is used to create both diagonal mass matrices and mixed mass matrices. © 1997 John Wiley & Sons, Ltd.

Int. J. Numer. Meth. Engng., **40**, 4259–4271 (1997)

No. of Figures: 15. No. of Tables: 1. No. of References: 13.

KEY WORDS: finite element method; mass matrix

1. INTRODUCTION

Mass matrices used in the finite element method can be derived in many different ways. In the early days of the finite element method, it was common to simply place particle masses, m_i, at nodes i of an element in such a way that $\sum m_i$ became the total element mass. These particle 'lumps' had no rotary inertia unless rotary inertia was arbitrarily assigned, as was sometimes done for the rotational degrees of freedom of beams and plates. This method of generating mass matrices, called *ad hoc lumping*, is probably the most intuitive of all lumping methods. Better lumping methods have been developed since then. One of the advantages of lumped mass matrices is that they are diagonal. This property can be utilized in many situations, in which they need to be inverted. For solving dynamic problems, there are also various time-stepping schemes for which a diagonal mass matrix is very advantageous.

A theoretically sounder approach to calculating the mass matrix than '*ad hoc* lumping' was introduced by Archer.[1] Although Archer made no explicit mention of the term 'finite element', he introduced a technique for calculating distributed mass influence matrices that is still in use today within the framework of the finite element method. Archer expressed structural velocities as the product of displacement interpolation functions and generalized velocities. Inserting this expression into the general formula for kinetic energy, he obtained a consistent mass matrix. When one speaks of a consistent mass matrix today, one usually refers to its having been calculated using the same shape functions as the stiffness matrix and as the other terms in the finite element equations. With the formulation of consistent mass matrices it was possible to establish convergence criteria for

* Correspondence to: Per-Anders Hansson, Division of Structural Mechanics, Lund University, PO Box 118, SE-221 00 Lund, Sweden

CCC 0029–5981/97/224259–13$17.50

Received 23 December 1996
Revised 30 April 1997

eigenvalues obtained from finite element equations. These criteria were found to represent the upper bounds of the exact solution.

Przemieniecki[2] showed that the concept of consistent mass matrix could be improved however, by using frequency-dependent shape functions to describe the structural motions. This idea was developed further by Gupta,[3] who generalized Przemieniecki's approach for two and three dimensions. Gupta's the so-called dynamic element method has the serious drawback, however, that it results in a quadratic eigenvalue problem which cannot be solved by means of standard numerical techniques. This disadvantage is probably a major reasons for the dynamic element method not coming into widespread use in the finite element community, although Gupta *et al.*[4] have described a technique for solution of quadratic matrix equations requiring approximately the same computing time as the standard linear eigenvalue problem. Despite this, the earlier conceptions of lumped and frequency-independent consistent mass matrices are still dominant in finite element analysis.

One way to obtain accuracy almost as great as that of frequency-dependent mass matrices is to combine a consistent mass matrix with a lumped mass matrix, preserving the mass by scaling the two matrices appropriately. This technique has shown to provide good results in eigenvalue analyses of many different element types, see References 5 and 6.

Although one might think that, because of its better theoretical foundations the consistent mass matrix would be the only type used in practice, such is not the case. As already indicated, there are time-stepping schemes such as the central difference method that require a diagonal mass matrix for their efficiency to be fully exploited. There are also cases in which a lumped mass matrix leads to better results than a consistent mass matrix does.

One of the simplest methods of obtaining a diagonal mass matrix is to sum all the entries in each row of the consistent mass matrix and to then store the sums in the corresponding diagonal matrix positions, the off-diagonal terms being set to zero. Although it is a simple method, this so-called row-sum technique has certain drawbacks: first that it cannot be applied to rotary mass terms, secondly, that it produces negative diagonal entries in the mass matrix if it is applied to elements having mid-side nodes, and thirdly that the whole consistent mass matrix must be computed first.

Another method of obtaining diagonal mass matrices is to use nodal quadrature integration rules. This involves using the nodes as integration points in the numerical integration scheme used to compute the mass matrix. Although this procedure has the advantage of generating no off-diagonal terms, it likewise has drawbacks. It generates block-diagonal mass matrices for elements with rotational degrees of freedom and, if used for elements having mid-side nodes, it generates negative entries in the diagonal. For other elements the method has been shown to have the same convergence rate as the consistent mass matrix, see References 7–9.

A method that always generates positive definite mass matrices was proposed by Hinton *et al.*[10] Their approach is to scale the diagonal entries of the consistent mass matrix in such a way that the total mass is preserved and to then insert these scaled masses into the diagonal of the lumped mass matrix.

Sauer, see Reference 11, has suggested a different way off computing a diagonal consistent mass matrix. His approach is to add a sort of bubble-function to the normal shape functions, a function so constructed that the off-diagonal terms in the mass matrix vanish when the numerical integration is performed. However, this method is only applicable to a limited number of elements, e.g. to isoparametric four node elements.

In the present study another possibility is suggested. This involves varying the diagonal entries in the lumped mass matrix so as to minimize the error present in the eigenfrequencies, or to minimize the error contained in some other measure, using a simple geometry. The mass matrix

configuration with the smallest error is then chosen. Each diagonal entry is linked with a node. Through isoparametric mapping these masses are scaled in a manner appropriate for a given element that is distorted.

2. PRESENTATION OF THE METHOD

The method just referred to can be used to generate optimized diagonal mass matrices for elements with quadratic shape functions, as well as optimized mixed mass matrices.

2.1. Diagonal mass matrices

One expresses the mass matrix here using a variable relevant to the mass distribution within the element, one solves a simple eigenvalue-problem with one element or a small number of elements in a simple geometry. This simple eigenvalue-problem has to be solved a number of times for each value of the mass scaling variable that controls the mass distribution within the element. The variable is varied over a range of values allowing an error curve for the mass variable ψ to be obtained. The error measure used here is the frequency error

$$\varepsilon_1 = \left(\sum_{i=1}^{N} \frac{|f_i - \bar{f}_i|}{|f_i|} \right) \Big/ N \tag{1}$$

where f_i is the analytical frequency, $\bar{f}_i$ the computed frequency, and N the number of eigenfrequencies considered.

This yields a curve in which the error measure is a function of the mass parameter ψ. From this curve the most appropriate mass matrix can be selected.

Due to the attempt being made here to optimize the mass matrix in the undeformed parent domain, the method is ineffective for linear elements. For such elements all standard methods give the same results, namely that each node has the same portion of mass associated with it.

For elements having quadratic shape-functions, on the other hand, the mass matrices that standard methods for mass lumping yield for various elements differ also in the parent domain. Accordingly since different portions of the mass can be associated with the various nodes it is meaningful to use a method of this sort to generate mass matrices, as the numerical examples will indicate.

The isoparametric mapping solves the problems connected with the scaling of the mass associated with each node. The transformation is performed on the area or volume that is lumped to a particular node, see Figure 1.

When dealing with linear elements, one can use these same principles, so as to create optimized mixed mass matrices instead, as is taken up in the next section.

2.2. Mixed mass matrices

Since consistent mass matrices overestimate the natural frequencies whereas lumped mass matrices usually underestimate them, a linear combination of the two can yield more satisfactory results. Let

$$\mathbf{M}_{\text{mix}} = \alpha \mathbf{M}_{\text{C}} + \beta \mathbf{M}_{\text{L}} \tag{2}$$

where α and β are the weighting parameters for the consistent and the lumped matrix, respectively.

$$\alpha + \beta = 1 \tag{3}$$

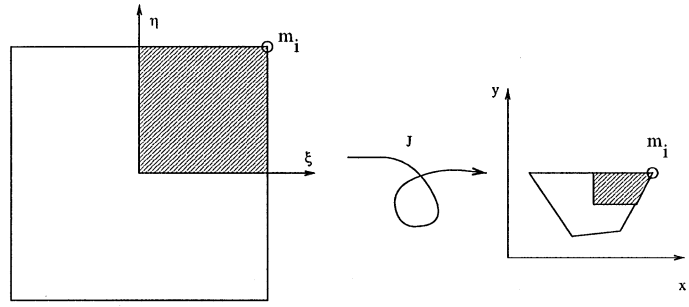

Figure 1. The mass associated with each node is proportional to the shaded area. This area is mapped to the global domain by isoparametric transformation

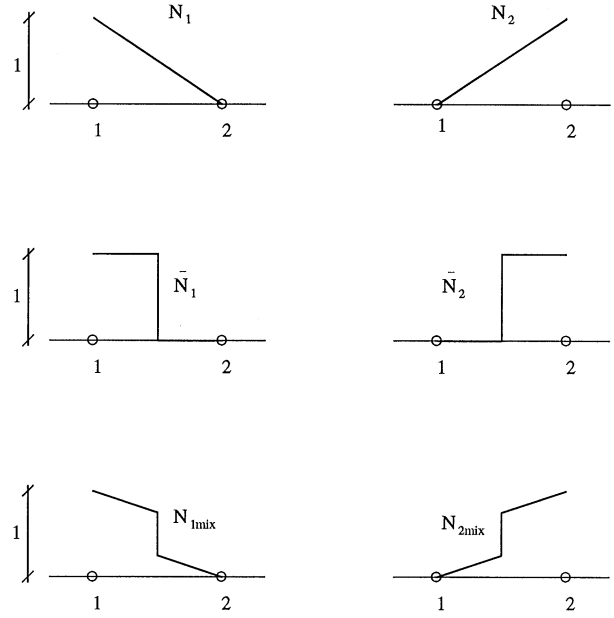

Figure 2. Shape functions for a linear bar element. Above is a consistent element, in the middle a lumped element and below a mixed element

This procedure can be seen as combining the shape-functions of each element from the consistent and the lumped matrix into a single function, see References 5 and 11. Various mixed shape functions for a linear bar element are shown in Figure 2.

Instead of using α and β, one can also express the mixed mass matrix as

$$\mathbf{M}_{\text{mix}} = (1-\gamma)\mathbf{M}_{\text{C}} + \gamma\mathbf{M}_{\text{L}} \tag{4}$$

where the formulation for the lumped mass matrix corresponds to $\gamma = 1$ and that for the consistent mass matrix to $\gamma = 0$. All other possible values of γ correspond to a 'mixed matrix'. The method of

minimization of the modal errors can be applied to mixed matrices through varying the parameter γ in equation (4).

3. NUMERICAL EXAMPLES

A comparison of different types of mass matrices will be presented in this section. The objective is not simply to examine how adequately the method that is suggested performs, but also to examine how adequately other methods behave.

In denoting the weighting parameters, ψ refers to diagonal matrices and γ to mixed matrices.

3.1. Diagonal matrices

In this section mass matrices for a one-dimensional quadratic bar element and a two-dimensional quadratic acoustic element are tested.

For a quadratic bar element with equal spacing between nodes, see Figure 3, the consistent and the lumped mass matrix, respectively, are

$$\mathbf{M}_c = \frac{\rho AL}{30}\begin{bmatrix} 4 & 2 & -1 \\ 2 & 16 & 2 \\ -1 & 2 & 4 \end{bmatrix} \tag{5}$$

$$\mathbf{M}_l = \frac{\rho AL}{6}\begin{bmatrix} 1 & 0 & 0 \\ 0 & 4 & 0 \\ 0 & 0 & 1 \end{bmatrix} \tag{6}$$

The lumped mass matrix can be expressed in a manner allowing the lumping to be varied. If the element mass is distributed at the nodes in the manner shown in Figure 3, the total element mass m is preserved if

$$\theta = 1 - 2\psi \tag{7}$$

Accordingly, the lumped mass matrix can also be written as

$$\mathbf{M}_l(\psi) = \rho AL\begin{bmatrix} \psi & 0 & 0 \\ 0 & 1-2\psi & 0 \\ 0 & 0 & \psi \end{bmatrix} \tag{8}$$

All the standard methods here yield $\psi = \frac{1}{6}$.

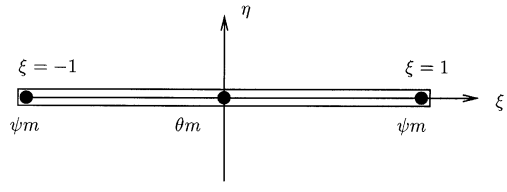

Figure 3. A three-node bar element with different masses associated with each node

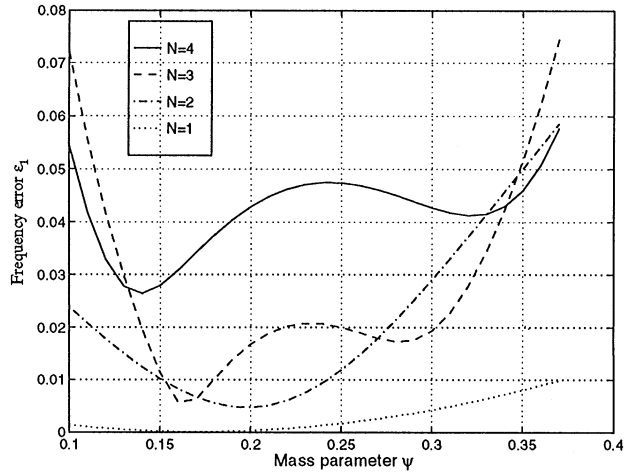

Figure 4. Frequency error, ε_1, for different number of eigenvalues, N, used in equation (1). The model involves of four degrees of freedom

As a numerical example involving this type of element, consider a bar with one end fixed and the other end free. An eigenvalue analysis of this system is performed using different types of mass matrices. The computed eigenvalues are compared then with the analytical ones.

The analytical eigenfrequencies for this problem are

$$\omega_i = \frac{\pi}{2L}\sqrt{\frac{E}{\rho}}(2i-1), \quad i = 1, 2, 3 \ldots \tag{9}$$

Note that the frequency error ε_1 varies with the matrix type, i.e. with differing values of ψ. The result is shown in Figure 4.

As can be seen, the frequency error ε_1 depends on the number of frequencies comprising the sum. If one is only interested in the fundamental frequency, the optimal ψ is the same as obtained for standard methods of lumping.

An eight-node isoparametric quadratic element is also examined. In searching for a parameter to express the mass matrix here, one should note that if the mass associated with every corner node in the parent domain is ψ, and the mass associated with every mid-side node is θ, the following condition must be satisfied

$$\theta = \frac{1-4\psi}{4} \tag{10}$$

The element and the areas associated with each node are shown in Figure 5. The shaded areas correspond to the corner node masses.

In endeavoring to optimize ψ for a single eight-node element, one obtains curves such as those shown in Figure 6. Different curves are obtained for the different values of N contained in equation (1). For $N = 1$, i.e. for the fundamental frequency, the curve has a minimum for $\psi = 0{\cdot}030$, the optimal value for $N = 4$ being $\psi = 0{\cdot}017$. If all the frequencies are used, i.e. for $N = 8$ the minimum is for $\psi = 0{\cdot}192$. For a single undistorted element, the special lumping technique yields $\psi = 0{\cdot}0278$ and the equal lumping technique $\psi = 0{\cdot}25$.

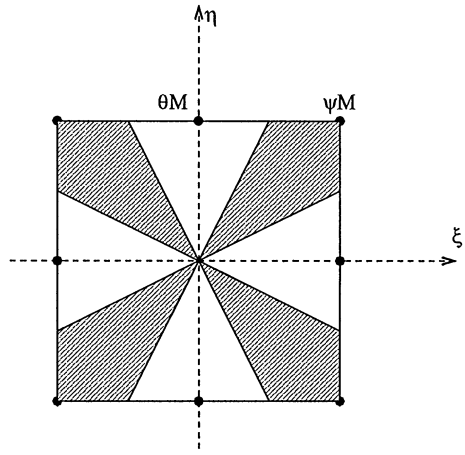

Figure 5. Allocation of N_i in a two-dimensional quadratic isoparametric element. Shaded area refers to $N_i = 1$ for the corner nodes, and white area refers to $N_i = 1$ for midside nodes

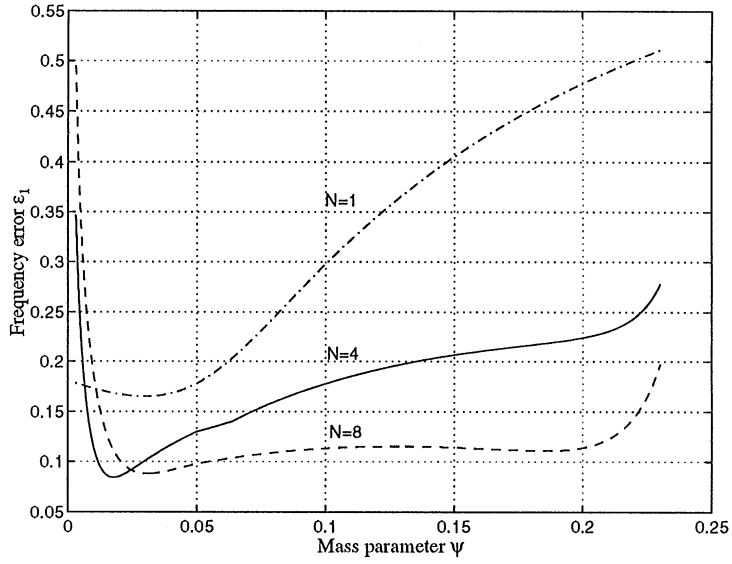

Figure 6. Errors in frequency vs. mass parameter ψ for a quadratic element

In Figure 7, a element with the mass configuration corresponding to $\psi = 0{\cdot}017$ is compared with elements obtained for other lumping schemes. As can be seen, the proposed lumping scheme in which $\psi = 0{\cdot}017$ has the best convergence rate of all the lumping methods. The special lumping scheme performs nearly as well. Equal lumping shows the worst performance of the methods tested here.

An eight-node element involving distortion is tested next, see Figures 8 and 9. All the methods are numerically stable when the mesh is distorted. An observation of interest is that when the

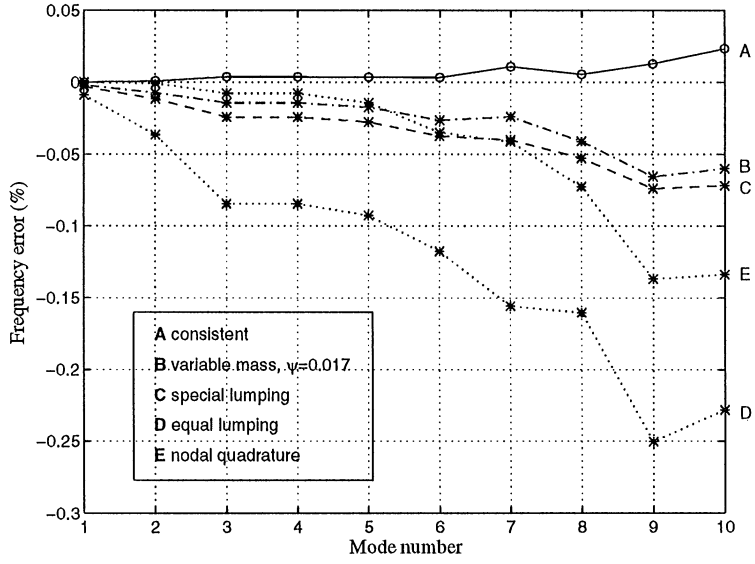

Figure 7. Error in frequency vs. mode number in a 12-element model

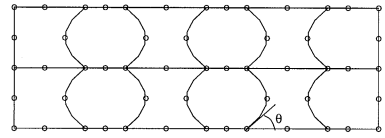

Figure 8. Mesh for 8-node distorted elements

distortion angle increases, the accuracy of the diagonal consistent method and of the special lumping method increases as well, see Figure 9.

How the number of elements per wavelength affects the error-curves is likewise investigated. In the curve for $N = 1$ in Figure 6, two elements are used per wavelength. Figure 10 in which curves for $N = 1$ are shown for different numbers of elements per wavelength, one observe that the minimum moves towards $\psi = 0$ when the number of elements is increased.

Thus, if the fundamental frequency is the dominant aspect of a problem, the proper choice of ψ would be $\psi = 0$. With this choice, one concentrates the masses in the midside nodes. The number of unknowns in the problem can then easily be reduced by means of static condensation.

3.2. Mixed matrices

As an illustrative example, consider a bar fixed at one end. First we note how the frequency error varies with the mode number for the different matrix types, see Figure 11. As expected, one can observe that the consistent mass matrix overestimates the eigenfrequency and that the lumped mass matrix underestimates it. The mixed matrix is somewhere in between. The shape of this curve varies with the weighting parameter γ, and also to some extent with the number of elements employed. As evident in the figure, the mixed matrix gives better results than either the consistent or the lumped mass matrix.

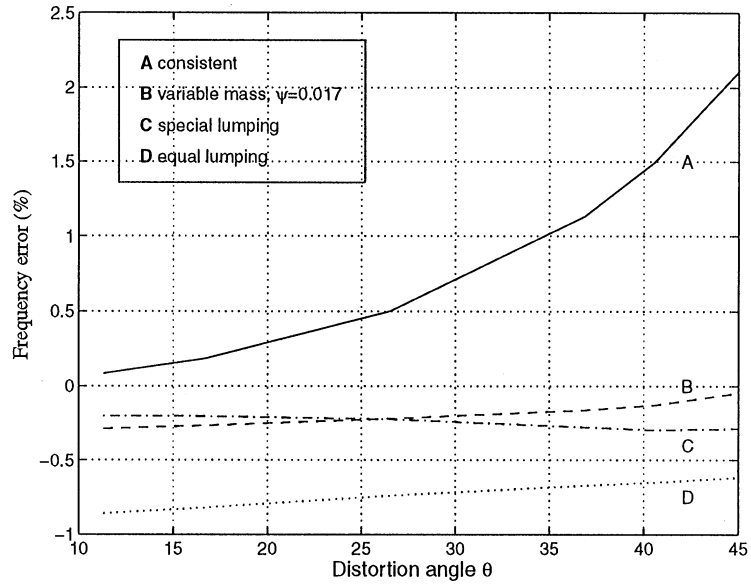

Figure 9. Frequency error vs. distortion angle for a quadratic 8-node element

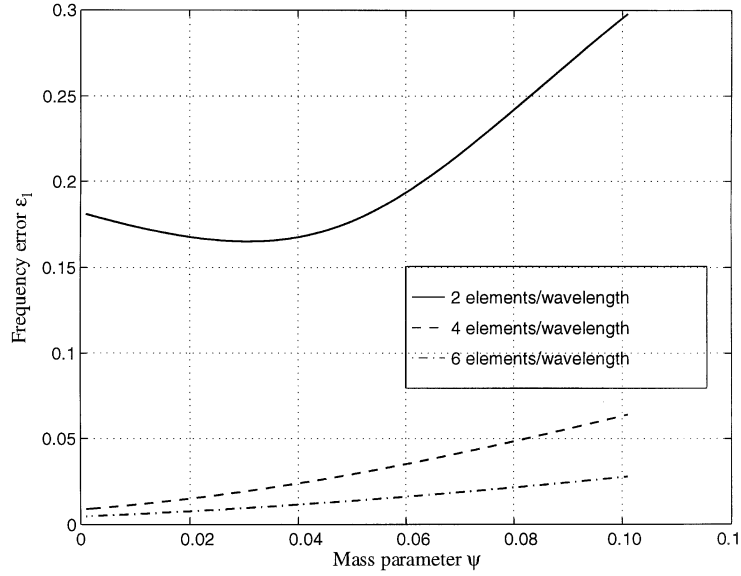

Figure 10. Error curve for different number of elements per wavelength for quadratic 8-node element

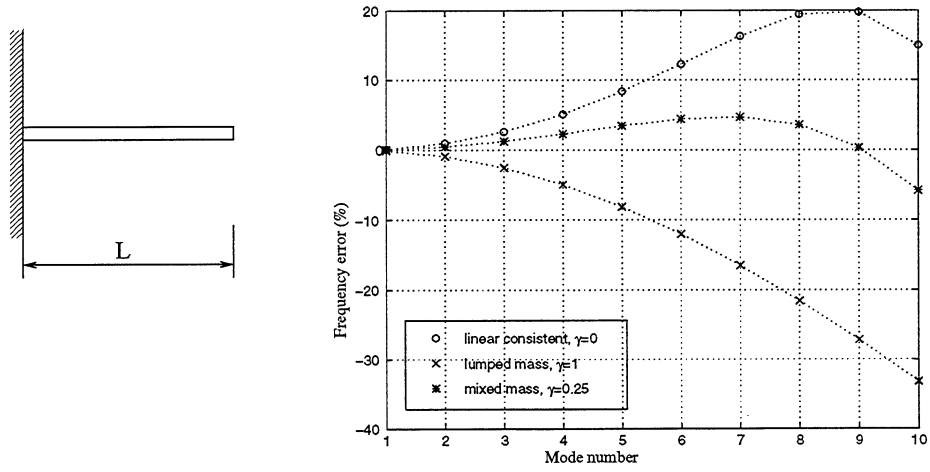

Figure 11. (a) Bar of length L, fixed at one end, and (b) Frequency error vs. mode number in a ten element model

Table I. Suggested configurations of mixed mass matrices for a linear bar element

Form	Value of γ
Lumped	1
Averaged	0·5
Ki-Ook Kim[5]	0·4
Stavrinidis *et al.*[6]	0·25
Consistent	0

Next, the dependency of the frequency error ε_1 on the parameter γ in a mixed matrix is examined. Note that for $N = 1$ the curve for the frequency error has a minimum at $\gamma \approx \frac{1}{4}$. For this element-type, the minimum can also be derived analytically, see Reference 6. Note also that the minimum of the error curve is dependent upon how many eigenvalues are used in the calculation of e.g. ε_1. In some cases, when only the lower eigenvalues are of interest, one can optimize the mass matrix to whatever number of eigenvalues is desired. Other authors have suggested values of γ in accordance with Table I. If one compares this table with Figure 12 one can observe that the values in Table I are in the range of 0·25–0·5, which is exactly where the curves in Figure 12 have their minima. It is important here that one knows which frequency range is of interest, since one can then choose a value for γ that suits one's needs.

The same type of tests that were made for the bar element can be carried out for the two-dimensional acoustic element. Observe first the error in the eigenfrequency vs. the mode-number, as shown in Figure 13.

Note here that a mixed matrix yields very satisfactory results compared with the lumped and the consistent mass matrix. The next matter to be examined is how the mass parameter γ in equation (4) can be optimized, see Figure 14.

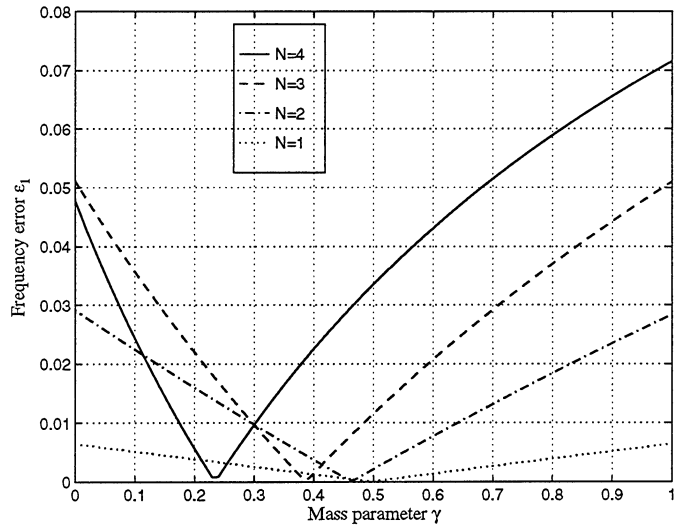

Figure 12. Summed frequency error ε_1 vs. the parameter γ in a model with four degrees of freedom

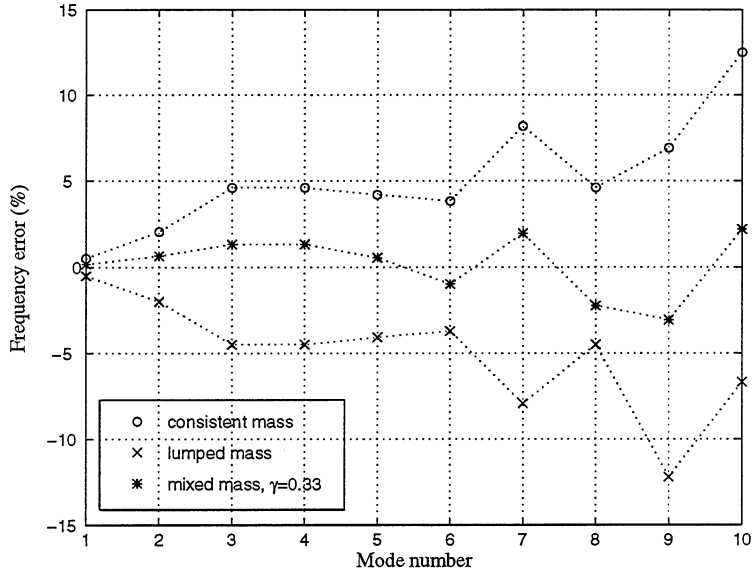

Figure 13. Errors in frequency vs. the mode number in a model with 27 two-dimensional acoustic elements

As can be seen here too, the number of frequencies used is a highly important factor in attempting to find the minimum on the error curve. The minima on the error curves range from 0·25 to 0·5.

The importance of the number of elements per wavelength is tested for this element type too. The results are shown in Figure 15.

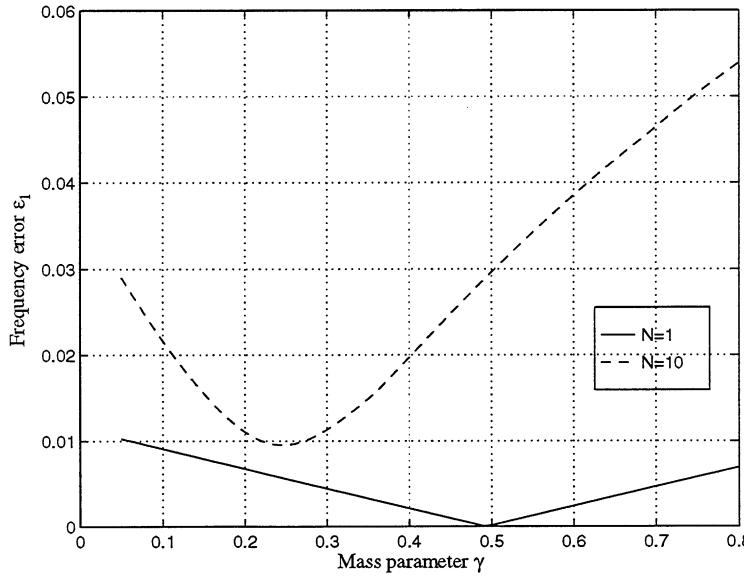

Figure 14. Errors in frequency vs. the mode mass parameter γ

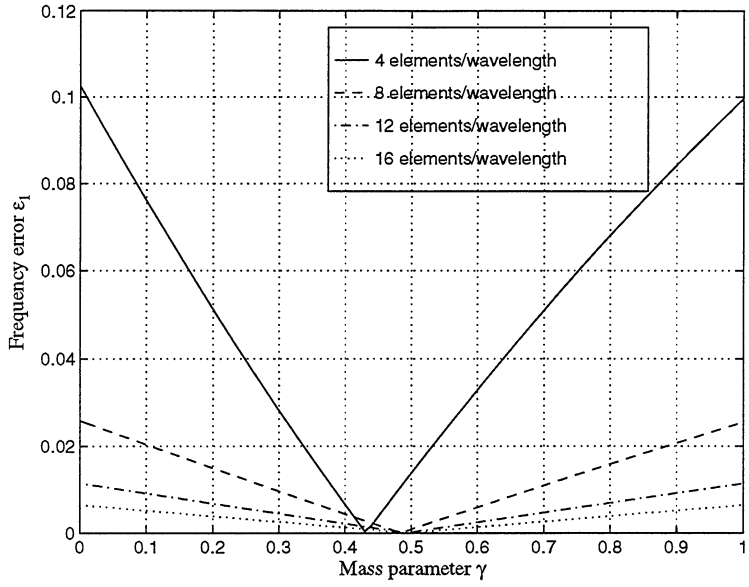

Figure 15. Error curve for different numbers of elements per wavelength for a linear 4-node element

As can be seen, the optimal γ changes from 0·45 to 0·5 when one increases the number of elements per wavelength from four to eight, the optimal γ remaining constant if still a greater number of elements is involved.

4. CONCLUSIONS

Different mass lumping methods have been described and tested numerically. The analytical eigenvalues were the target of these tests. A new method for constructing mass matrices was outlined, one involving the obtaining of mass matrices by the minimization of modal errors, allowing one to construct a mass matrix optimized for the frequency range of interest. This method has been used to construct both mixed mass matrices and lumped diagonal mass matrices. The proposed method was found to perform well, compared with other methods for constructing diagonal lumped mass matrices. The characteristics of the diagonal mass matrix obtained by use of method are often very close to those of the matrix obtained by the special lumping technique described by Hinton, Rock and Zienkiewicz. The present method is very stable and performs well in all the situations for which it was tested.

Many suggestions concerning how to construct mixed mass matrices have been made in the literature. Using the approach suggested here, an optimized mass matrix can be obtained *for the frequency range of interest*. The numerical examples show too that mixed mass matrices perform very well as compared with consistent and lumped mass matrices.

It is important to note that the optimal value of the mass matrix depends on the number of elements per wavelength. For mixed matrices, the optimal γ-value changes by a few percent when the number of elements per wavelength is changed, its remaining constant when the number of elements per wavelength is increased beyond eight. For quadratic elements however, the optimal value of ψ goes towards zero when the number of elements is increased. Thus if the fundamental frequency is the dominant aspect of a problem, $\psi = 0$ could be employed, this concentrating the mass on the midside nodes. By performing static condensation then the size of the problem can be decreased.

REFERENCES

1. J. S. Archer, 'Consistent mass matrix for distributed mass systems', *J. Struct. Div. ASCE*, **89** (ST 4), 161–178 (1963).
2. J. S. Przemieniecki, *Theory of Matrix Structural Analysis*, McGraw-Hill, New York, 1985.
3. K. K. Gupta, 'Development of a solid hexadron finite dynamic element', *Int. J. Numer. Meth. Engng.*, **20,** 2143–2150 (1984).
4. K. K. Gupta, C. L. Lawson and A. R. Ahmadi, 'On the development of a finite dynamic element and solution by associated eigenproblem by a block Lanczos procedure', *Int. J. Numer. Meth. Engng.*, **33,** 1611–1623 (1992).
5. K. Kim, 'A review of mass matrices for eigenproblems', *Comput. Struct*., **46,** 1041–1049 (1993).
6. C. Stavrinidis, J. Clinckemaillie and J. Dubois, 'New concepts for finite-element mass matrix formulations', *AIAA J.*, **27,** 1249–1255 (1989).
7. I. Fried and D. Malkus, 'Finite element mass lumping by numerical integration with no convergence rate loss', *Int. J. Solids Struct.*, **11,** 461–466 (1975).
8. D. Malkus and M. Plesha, 'Zero and negative masses in finite element vibration and transient analyses', *Comput. Meth. Appl. Mech. Engng.*, **59,** 281–306 (1986).
9. D. Malkus, X. Qui, 'Divisor structure of finite element eigenproblems arising from negative and zero masses', *Comput. Meth. Appl. Mech. Engng.*, **66,** 365–368 (1988).
10. E. Hinton, T. Rock and O. C. Zienkiewicz, 'A note on mass lumping and related processes in the finite element method', *Earthquake Engng. Struct. Dyn.*, **4,** 245–249 (1975).
11. G. Sauer, 'Consistent diagonal mass matrices for the isoparametric 4-node quadrilateral and 8-node hexadron elements', *Commun. Numer. Meth. Engng.*, **9,** 35–43 (1993).
12. O. C. Zienkiewicz and R. L. Taylor, *The Finite Element Method*, Prentice-Hall, Englewood Cliffs, N.J., 1989.
13. G. Strang and G. J. Fix, *An Analysis of the Finite Element Method*, 4th ed., Vol.1., McGraw-Hill, London, 1973.

Paper 2

Domain Decomposition in Acoustic and Structure-Acoustic Analysis

G. Sandberg, P-A. Hansson, M. Gustavsson

Computer methods in applied mechanics and engineering, 190, 2979-2988(2001)

Paper 3

A SYMMETRIC TIME-STEPPING SCHEME FOR COUPLED PROBLEMS

P-A. WERNBERG, G. SANDBERG

WCCM V CONGRESS IN VIENNA (2002)

WCCM V
Fifth World Congress on
Computational Mechanics
July 7–12, 2002, Vienna, Austria
Eds.: H.A. Mang, F.G. Rammerstorfer,
J. Eberhardsteiner

A symmetric time-stepping scheme for coupled problems

P.A. Wernberg*, G. Sandberg

Division of Structural Mechanics
Lund University, PO Box 118,221 00 Lund, Sweden
e-mail: wernberg@byggmek.lth.se

Key words: Fluid-structure interaction,coupled problems,implicit,time-stepping

Abstract
In a particular class of coupled problems, the resulting coupled set of equations is unsymmetrical. In this paper a simple procedure for introducing a symmetric effective stiffness matrix using implicit time stepping procedures in fluid-structure problems, is proposed. As long as the time step is kept constant, the factorization of the effective stiffness matrix only needs to be performed once. The numerical example show that cpu time and memory utilization decreases with the proposed formulation.

1 Introduction

There is a class of coupled problems that result in an unsymmetrical system of equations.The reason for this, although the complete system is conservative, is how the information is passed between the two domains. The unsymmetrical representation is the most compact representation of the coupled system possible. However, the unsymmetrical system doubles the demand for storing the system matrices and also double the number of operations to be performed for a specific analysis. Hence, there is a benefit in reformulating the system creating a symmetric representation. In a previous work, see [1], this has been done for the coupled eigenvalue problem.

The interacting fluid-structure problem for the structural domain can be written

$$\mathbf{M}_s\ddot{\mathbf{d}} + \mathbf{C}_s\dot{\mathbf{d}} + \mathbf{K}_s\mathbf{d} - \mathbf{H}_{fs}\mathbf{p} = \mathbf{f}_b \tag{1}$$

where

$$\begin{aligned} \mathbf{M}_s &= \int_{V_s} \mathbf{N}_s^T \rho_s \mathbf{N}_s \, dV \qquad & \mathbf{K}_s &= \int_{V_s} (\widetilde{\nabla}\mathbf{N}_s)^T \mathbf{D} \widetilde{\nabla}\mathbf{N}_s \, dV \\ \mathbf{H}_{fs} &= \int_S \mathbf{N}_s^T \cdot \mathbf{n}\mathbf{N}_f \, dS \qquad & \mathbf{f}_b &= \int_{V_s} \mathbf{N}_s^T \rho_s \mathbf{b} \, dV \end{aligned} \tag{2}$$

and $\mathbf{N}_s$ is a polynomial matrix, for the structural domain V_s. All the matrices above, including the damping matrix $\mathbf{C}_s$, are considered to be symmetrical.

For the fluid domain, V_f, we have

$$\mathbf{M}_f\,\ddot{\mathbf{p}} + \mathbf{C}_f\dot{\mathbf{p}} + \mathbf{K}_f\,\mathbf{p} + \mathbf{H}_{sf}\ddot{\mathbf{d}} = \mathbf{f}_q \tag{3}$$

where

$$\begin{aligned} \mathbf{M}_f &= \int_{V_f} \mathbf{N}_f^T \mathbf{N}_f \, dV \qquad & \mathbf{K}_f &= \int_{V_f} (\nabla\mathbf{N}_f)^T c^2 \nabla\mathbf{N}_f \, dV \\ \mathbf{H}_{sf} &= \int_S \mathbf{N}_f^T \rho c^2 \mathbf{N}_s \, dS \qquad & \mathbf{f}_q &= \int_{V_f} \mathbf{N}_f^T c^2 \dot{q} \, dV \end{aligned} \tag{4}$$

and $\mathbf{N}_f$ is a polynomial matrix, for the fluid domain V_f. q is the mass inflow per unit volume and time.All the matrices above, including the damping matrix $\mathbf{C}_f$, are considered to be symmetrical. Putting these equations together, and introducing

$$\begin{aligned} \mathbf{H}_{fs} &= \mathbf{H} \\ \mathbf{H}_{sf} &= \rho c^2 \mathbf{H} \end{aligned} \tag{5}$$

we get the following unsymmetrical system of equations

$$\begin{bmatrix} \mathbf{M}_s & 0 \\ \rho c^2\,\mathbf{H}^T & \mathbf{M}_f \end{bmatrix} \begin{bmatrix} \ddot{\mathbf{d}} \\ \ddot{\mathbf{p}} \end{bmatrix} + \begin{bmatrix} \mathbf{C}_s & 0 \\ 0 & \mathbf{C}_f \end{bmatrix} \begin{bmatrix} \dot{\mathbf{d}} \\ \dot{\mathbf{p}} \end{bmatrix} + \begin{bmatrix} \mathbf{K}_s & -\mathbf{H} \\ 0 & \mathbf{K}_f \end{bmatrix} \begin{bmatrix} \mathbf{d} \\ \mathbf{p} \end{bmatrix} = \begin{bmatrix} \mathbf{f}_b \\ \mathbf{f}_q \end{bmatrix} \tag{6}$$

2 Reformulating for symmetric time integration

Introducing the multiplication factor α into the second line of equations in Eq. 6 yields

$$\begin{bmatrix} \mathbf{M}_s & 0 \\ \alpha\rho c^2\,\mathbf{H}^T & \alpha\mathbf{M}_f \end{bmatrix}\begin{bmatrix} \ddot{\mathbf{d}} \\ \ddot{\mathbf{p}} \end{bmatrix}+\begin{bmatrix} \mathbf{C}_s & 0 \\ 0 & \alpha\mathbf{C}_f \end{bmatrix}\begin{bmatrix} \dot{\mathbf{d}} \\ \dot{\mathbf{p}} \end{bmatrix}+\begin{bmatrix} \mathbf{K}_s & -\mathbf{H} \\ 0 & \alpha\mathbf{K}_f \end{bmatrix}\begin{bmatrix} \mathbf{d} \\ \mathbf{p} \end{bmatrix}=\begin{bmatrix} \mathbf{f}_b \\ \alpha\mathbf{f}_q \end{bmatrix} \tag{7}$$

Now consider a standard implicit time integration scheme

1. Initialize, $\mathbf{u}_0$, $\dot{\mathbf{u}}_0$, $\ddot{\mathbf{u}}_0$
2. Form the effective stiffness matrix, $\mathbf{K}_{eff} = \mathbf{M}/\beta\left(\Delta t\right)^2 + \gamma\mathbf{C}/\beta\Delta t + \mathbf{K}$
3. Factorize $\mathbf{K}_{eff} = \mathbf{L}\mathbf{D}\mathbf{L}^T$.

   For each time step perform the following steps

   (a) Evaluate the effective forces
   $\mathbf{f}_{eff} = \mathbf{f}_{n+1} - \mathbf{M}\left(\mathbf{u}_n/\beta\left(\Delta t\right)^2 + \dot{\mathbf{u}}_n/\beta\Delta t + \ddot{\mathbf{u}}_n\left(1-2\beta\right)/2\beta\right)$

   (b) Solve $\mathbf{L}\mathbf{D}\mathbf{L}^T\mathbf{a} = \mathbf{f}_{eff}$.

   (c) Calculate the accelerations and velocities at the new timestep.

The crucial part of the scheme is the factorization of the effective stiffness matrix In this case the effective stiffness matrix according to Eq. 7 and step (2) is

$$\mathbf{K}_{eff} = \begin{bmatrix} \mathbf{K}_s + \frac{1}{\beta(\Delta t)^2}\mathbf{M}_s + \frac{\gamma}{\beta\Delta t}\mathbf{C}_s & -\mathbf{H} \\ \frac{\alpha\rho c^2}{\beta(\Delta t)^2}\mathbf{H}^T & \alpha\mathbf{K}_f + \frac{\alpha}{\beta(\Delta t)^2}\mathbf{M}_f + \frac{\alpha\gamma}{\beta\Delta t}\mathbf{C}_f \end{bmatrix} \tag{8}$$

Based on the original system , $\alpha = 1$, the effective stiffness matrix is not symmetric and hence symmetric solvers can not be utilized. The matrix can be made symmetric, however , if

$$\alpha = -\frac{\beta\left(\Delta t\right)^2}{\rho c^2} \tag{9}$$

For this choice of α the system matrix becomes

$$\mathbf{K}_{eff} = \begin{bmatrix} \mathbf{K}_s + \frac{1}{\beta(\Delta t)^2}\mathbf{M}_s + \frac{\gamma}{\beta\Delta t}\mathbf{C}_s & -\mathbf{H} \\ -\mathbf{H}^T & -\frac{\beta(\Delta t)^2}{\rho c^2}\mathbf{K}_f - \frac{1}{\rho c^2}\mathbf{M}_f - \frac{\gamma\Delta t}{\rho c^2}\mathbf{C}_f \end{bmatrix} \tag{10}$$

The time step enters into the efficient stiffness matrix, and as long as the time step is kept constant, the same factorization can be used.

3 Other formulations

In [3], Sandberg and Göransson proposed a symmetric three field form, by introducing a fluid displacement potential, $\mathbf{\Psi}$.

$$\begin{bmatrix} \mathbf{M}_s & 0 & 0 \\ 0 & \frac{\rho}{c^2}\mathbf{K}_f & 0 \\ 0 & 0 & 0 \end{bmatrix} \begin{bmatrix} \ddot{\mathbf{d}} \\ \ddot{\Psi} \\ \ddot{\mathbf{p}} \end{bmatrix} + \begin{bmatrix} \mathbf{K}_s & 0 & -\mathbf{H} \\ 0 & 0 & \frac{1}{c^2}\mathbf{K}_f \\ -\mathbf{H}^T & \frac{1}{c^2}\mathbf{K}_f & -\frac{1}{\rho c^2)}\mathbf{M}_f \end{bmatrix} \begin{bmatrix} \mathbf{d} \\ \Psi \\ \mathbf{p} \end{bmatrix} = \begin{bmatrix} \mathbf{f}_b \\ 0 \\ \mathbf{f}_q \end{bmatrix} \tag{11}$$

The drawback for this formulation, however, is that it demands twice as many degrees of freedom for the fluid part compared to Eq. 6. Another possibility proposed in [4] by Everstine is a symmetric two field formulation. This is accomplished by introducing a fluid velocity potential, $\mathbf{\Phi}$.

$$\mathbf{\Phi} = \dot{\Psi} \tag{12}$$

This leads to

$$\begin{bmatrix} \mathbf{M}_s & 0 \\ 0 & -\frac{\rho}{c^2}\mathbf{M}_f \end{bmatrix} \begin{bmatrix} \ddot{\mathbf{d}} \\ \ddot{\Phi} \end{bmatrix} + \begin{bmatrix} \mathbf{C}_s & \rho\mathbf{H} \\ \rho\mathbf{H}^T & \mathbf{M}_f \end{bmatrix} \begin{bmatrix} \dot{\mathbf{d}} \\ \dot{\Phi} \end{bmatrix} + \begin{bmatrix} \mathbf{K}_s & 0 \\ 0 & -\frac{\rho}{c^2}\mathbf{K}_f \end{bmatrix} \begin{bmatrix} \mathbf{d} \\ \Phi \end{bmatrix} = \begin{bmatrix} \mathbf{f}_b \\ -\frac{\rho}{c^2}\mathbf{F}_q \end{bmatrix} \tag{13}$$

The drawback here is that it leads to a quadratic eigenvalue problem even in the non-damped case. In the transient case, with a implicit time stepping scheme, it leads to the following effective system matrix

$$\mathbf{K}_{eff} = \begin{bmatrix} \mathbf{K}_s + \frac{1}{\beta(\Delta t)^2}\mathbf{M}_s + \frac{\gamma}{\beta\Delta t}\mathbf{C}_s & \frac{\gamma}{\beta\Delta t}\rho\mathbf{H} \\ \frac{\gamma}{\beta\Delta t}\rho\mathbf{H}^T & -\frac{c^2}{\rho}\mathbf{K}_f - \frac{c^2}{\rho\beta(\Delta t)^2}\mathbf{M}_f + \frac{\gamma}{\beta\Delta t}\mathbf{C}_f \end{bmatrix} \tag{14}$$

There are several other possible formulations of the coupled acoustic fluid-structure problem. For a survey see e.g [5]. In the numerical example, however, the formulations in Eq. 8, 10 and 14 are used.

4 Numerical example

Consider a three dimensional cavity with a flexible plate on the top, Figure 1.

A transient load is applied to the structure according to Figure 2.

The computer implementation of this problem is done in fortran. The SGI math libraries, SCSL [6], are used to factorize and solve the equations. The solvers used, psldlt and psldu, are direct solvers for sparse matrices. The pressure in the fluid in one of the smaller meshes can be seen in Figure 3.

The numerical results for the different formulations, unsymmetrical Eq. 6, symmetric according to Everstine Eq. 13 and the proposed symmetric system Eq. 7 can be seen in Table 4

The effective stiffness matrix K_{eff} is positive definite in the symmetrical case and indefinite in the unsymmetrical cases.

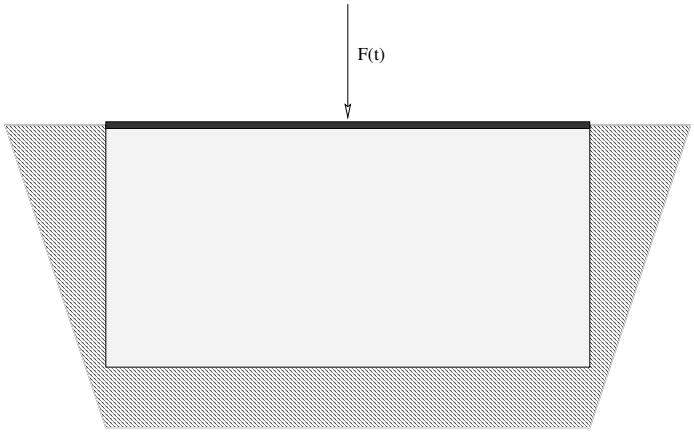

Figure 1: Cavity size: 12*6*6. *Structural properties*: $E = 70e9 \quad t = 0.064 \quad v = 0.3 \quad \rho = 2690$ *Fluid properties*: $\rho = 1.21 \quad c = 340$

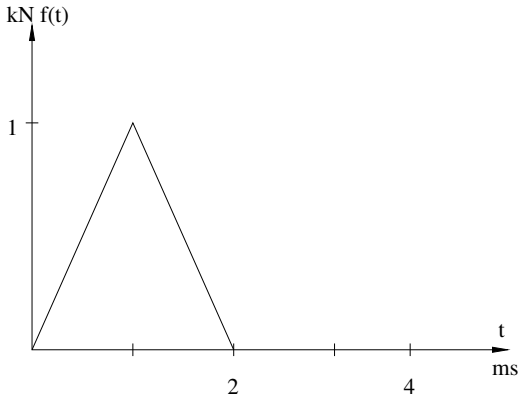

Figure 2: Transient load applied to the plate, $F_{max} = 1000 * g$

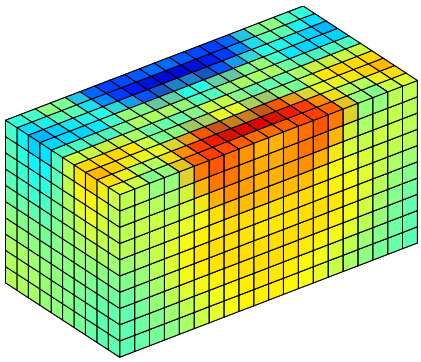

Figure 3: Fluid pressure in cavity after 1ms

Table 1: Numerical results. Time for time-step loop.

Method	3234 dofs	20664 dofs	64294 dofs	146124 dofs
unsymmetrical form, Eq. 8, SCSL ldu	7.21	90.7	564	2427
symmetrical form, Eq. 10 , SCSL ldlt	6.02	68.7	346	1338
symmetrical form, Eq. 14, SCSL ldlt	6.09	68.4	361	1401

5 Conclusions

A symmetric time stepping scheme for unsymmetrical problems has been evaluated. Both numerical results and theoretical considerations shows that the proposed method is faster and need less memory than if one should solve the unsymmetrical problem directly. The method has proven to be stable in the numerical examples.

Acknowledgements

All computations are on done on a SGI Origin 2000 machine, hosted by LUNARC at Lund University. LUNARC is gratefully acknowledged for this.

References

[1] G. Sandberg, *A new strategy for solving fluid-structure problems.*, Int J Numer Methods Eng., 38, (1995), 357–370.

[2] *Calfem, A finite element toolbox to MATLAB*, Division of Structural Mechanics and Division of Solid Mechanics, Lund Institute of Technology, Lund, Sweden (1999).

[3] G. Sandberg, P. Göransson, *A symmetric finite element formulation for acoustic fluid-structure interaction analysis*, J. Sound Vib., 123, (1988), 507–516.

[4] G. C. Everstine, *A symmetric potential formulation for fluid-structure interaction* , J. Sound Vib., 79, (1981), 167–160.

[5] H. Carlsson *Finite element analysis of structure-acoustic systems; formulations and solution strategies.*, Doctoral Thesis, Division of Structural Mechanics, Lund Institute of Technology, Lund, Sweden (1992).

[6] SCSL. *SGI's Scientific Computing Software Library (SCSL)*, http://techpubs.sgi.com.

Paper 4

Dynamic Finite Element Analysis of Fluid-filled Pipes

P-A. Hansson and G. Sandberg

Computer methods in applied mechanics and engineering, 190, 3111-3120(2001)

Paper 5

ANALYSIS OF SOUND TRANSMISSION LOSS OF DOUBLE-LEAF WALLS IN THE LOW-FREQUENCY RANGE USING THE FINITE ELEMENT METHOD

P. DAVIDSSON, J. BRUNSKOG, P-A. WERNBERG, G. SANDBERG AND P. HAMMER

BUILDING ACOUSTICS, 11, 239-257(2004)

Paper 6

THE FINITE ELEMENT METHOD AS A DESIGN INSTRUMENT FOR ROOM ACOUSTICAL ENVIRONMENT

P-A. WERNBERG, G. SANDBERG

REPORT TVSM-7144, DIVISION OF STRUCTURAL MECHANICS, LUND UNIVERSITY(2006)

The Finite Element Method as a design instrument for room acoustical environment.

P-A. Wernberg, G. Sandberg
Division of Structural Mechanics
Lund University, Lund, Sweden
e–mail: wernberg@byggmek.lth.se

1 Introduction

Sound insulation of buildings becomes more and more important. Living in a noisy environment requires a quiet place to be able to e.g. work. Unfortunately, planners design is often not focused on the acoustical properties of a building. Constructive and aesthetic constraints take center stage in the state of design. As a consequence, people often have to live under acoustically unsatisfactory circumstances or have to improve the situation by a reconstruction of the building. A possibility to overcome this problem is the development of numerical tools that predict the acoustical behavior of a designed building. Such a tool has to represent the complex mechanisms of sound propagation in and through different materials and components. With such a tool the planner can determine the effects of constructive modifications on the sound insulation and the sound fields in a building realistically and efficiently.

There are two commonly used ways of studying the room acoustic properties. The first is to describe the phenomena by sound particles. This theory assumes a diffuse sound field and continuous absorbtion of sound at boundaries. The geometric approach was first proposed by Sabine [1], and is concerned with the statistical characteristics (diffusiveness) of the acoustic conditions present. With use of such a model he was able to describe acoustic conditions in terms of separate numerical quantities, such as reverberation time and absorption area. In the 1960s, ideas of this sort within structural acoustics were extended to different groups of resonance systems being distinguished, an approach referred to as SEA (Statistical Energy Analysis). However, these methods cannot be applied at low frequencies because of the low mode density.

While the geometric approach is good for a rough understanding of the sound field in a room, a more detailed understanding requires the use of wave theory, which allows for wave motion and the response of the room to be visualized in terms of a large number of normal modes, each behaving as a damped oscillator. A comprehensive study of this approach was taken by Morse and Feshbach [2], who successfully applied this method to room acoustics. As they worked with closed form solutions, they only obtained solutions for highly idealized cases.

Architectural acoustics has long been concerned with the development of a high degree of precision in the assessment of both momentary and average acoustic conditions, also measures with relevance from a psychological standpoint. The measures involved concern such concepts as reverberation time and audibility, and questions of how sounds are

perceived under various conditions. For the low frequency area however, the models available today do not yield the degree of precision and differentiation required for achieving the level of sound-quality assessment that is needed. The use of finite element analysis allows for more complex geometries to be considered, and for various types of absorption at the bounding walls.

The finite element method is a general tool for solving differential equations. In many areas, such as the car industry , aeroplane industry and the space industry, it is considered as a natural part of the design process when developing new products, and also making modifications to existing products. Each of these areas has developed its own methodologies to be able to predict the behavior of the final product at an early stage in the design process. Numerical analysis is combined with experimental data from prototypes, and these experimental data is also a source to further develop the numerical models. This type of design process is not so well developed within the building industry. The are many reasons for this. But there are certainly possibilities to develop this kind of design process within industrialised construction. Both in terms of developing general components and the development of a specific construction.

The possibilities that an increased resolution in the analysis results creates, could also lead to new designs. Some of these possible analysis strategies in room acoustic situations will be presented here in of a couple of examples.

2 Numerical model

2.1 Finite element formulation of the acoustic equations

The finite element analysis of acoustic systems has been conducted be several researcher, e.g. Craggs [3] and Petyt [4]. Also in room acoustic situations it has been used as a way to determine the sound field. The nonhomogeneous wave equation expressed in terms of dynamic pressure p_d, is

$$\frac{\partial^2 p_d}{\partial^2 t} - c^2 \nabla^2 p_d = c^2 \frac{\partial^2 q}{\partial^2 t} \tag{1}$$

The application examples presented in the next section are all analyzed with a steady-state acoustic load therefore we assume harmonic motion and rewrite the equation as

$$\nabla p_d + k^2 p_d = -i\omega\rho_0 q \tag{2}$$

where

$$k = \frac{\omega}{c} \tag{3}$$

The boundary conditions applicable on the acoustic cavity are,
Imposed normal velocity on Ω_v:

$$v = \bar{v}_n \tag{4}$$

Imposed impedance on Ω_Z:

$$\frac{p}{v} = Z \tag{5}$$

Flexible wall:

$$u_s|_n = u_f|_n = -\frac{\partial p}{\partial n} \tag{6}$$

The finite element formulation of Eq. 1 is derived. This leads to the following matrix equation

$$\mathbf{K}_f\mathbf{p} + i\omega\mathbf{C}_f\mathbf{p} - \omega^2\mathbf{M}_f\mathbf{p} = \mathbf{f}_q + \mathbf{f}_v \tag{7}$$

where

$$\mathbf{M}_f = \int_{\Omega_f} \frac{1}{c^2}\mathbf{N}^T\mathbf{N}dV \tag{8}$$

$$\mathbf{K}_f = \int_{\Omega_f} \nabla\mathbf{N}\nabla\mathbf{N}dV \tag{9}$$

$$\mathbf{C}_f = \int_{\partial\Omega_Z} \rho_0\frac{1}{\bar{Z}}\mathbf{N}^T\mathbf{N}dS \tag{10}$$

$$\mathbf{f}_v = -\int_{\partial\Omega_v} i\rho_0\omega\mathbf{N}\bar{v}\mathbf{n}dS \tag{11}$$

$$\mathbf{f}_q = \int_{\Omega_f} i\rho_0\omega\mathbf{N}qdV \tag{12}$$

Investigations regarding the reduction of structure acoustic systems has been has been done by Sandberg, Wernberg and Davidsson, see e.g. [5]. These techniques will also be used here.

2.2 Porous sound absorbing material

In the application examples the damping material is modelled with a equivalent fluid model. In these models, the sound propagation in the porous material is described by the acoustic equation (1) with $\tilde{c}$, the speed of sound, calculated by

$$\tilde{c} = \sqrt{\frac{\tilde{K}}{\tilde{\rho}}} \tag{13}$$

where $\tilde{\rho}$ is the density and $\tilde{K}$ is the bulk modulus. These parameters are complex and frequency dependent.

When describing porous materials using an equivalent fluid model, the volume displacements in the fluid can be used. The actual fluid displacements in the pores, $\mathbf{u}_f$, are related to the volume displacements through the porosity, ϕ,

$$\mathbf{u}_{fv} = \phi\mathbf{u}_f \tag{14}$$

This gives simplified expressions in the boundary conditions.

The structural frame of the porous material is either considered to be rigid or limp and here a rigid model will be used.

This model is based on describing the sound propagation in porous materials as propagation of sound in cylindrical tubes with the frame considered rigid. A detailed description of this model was presented by Allard [6]. The frequency dependent density and bulk modulus are derived by including the viscosity of the air and the thermal exchange with the connecting frame in the model. The density of the porous material is given by

$$\tilde{\rho}(\omega) = \alpha_\infty \rho_0 \left[1 + \frac{\sigma\phi}{\mathrm{i}\omega\rho_0\alpha_\infty} G_J(\omega)\right] \tag{15}$$

and the bulk modulus

$$\tilde{K}(\omega) = \frac{\gamma P_0}{\gamma - (\gamma - 1)\left[1 + \frac{\sigma'\phi}{\mathrm{i}\mathrm{Pr}\omega\rho_0\alpha_\infty} G'_J(\mathrm{Pr}\omega)\right]^{-1}} \tag{16}$$

with

$$G_J(\omega) = \left[1 + \frac{4\mathrm{i}\alpha_\infty^2\eta\rho_0\omega}{\sigma^2\Lambda^2\phi^2}\right]^{1/2} \tag{17}$$

and

$$G'_J(\mathrm{Pr}\omega) = \left[1 + \frac{4\mathrm{i}\alpha_\infty^2\eta\rho_0\omega\mathrm{Pr}}{\sigma'^2\Lambda'^2\phi^2}\right]^{1/2} \tag{18}$$

where

$$\sigma' = \frac{\Lambda^2}{\Lambda'^2}\sigma \tag{19}$$

The density and bulk modulus are derived from the fluid displacements in the pores. Using the volume displacements, the density and the bulk modulus becomes

$$\begin{aligned} \tilde{\rho}_v(\omega) &= \frac{\tilde{\rho}(\omega)}{\phi} \\ \tilde{K}_v(\omega) &= \frac{\tilde{K}(\omega)}{\phi} \end{aligned} \tag{20}$$

with $\tilde{\rho}(\omega)$ and $\tilde{K}(\omega)$ from equations (15) and (16).

2.3 Stochastic simulations

Nowadays elaborate deterministic numerical methods and models, including sophisticated strategies for dealing with a variety of mechanical processes, have become wide-spread and are employed in everyday engineering design practice. However, in most design cases

the engineer is left with uncertainties about how to actually model a structure. The uncertainties can be directed towards the stiffness values of structural members or connections, geometrical or material properties. Production errors or damage, caused by accidents or inadequate management, are in many civil engineering structures uncertain parameters that should be considered in the analysis as well. Other issues are how the load is applied and, in dynamic analysis, the time history of the load.

There is a growing realization that unavoidable uncertainties must be considered in a computational scheme to produce reliable computational and engineering results. Traditionally, designers have used safety factors to provide increased confidence in the structural performance, but this approach does not take into account the special probability characteristics of a particular structure and does not provide the designer with adequate information about the reliability of the entire system. This has lead to rather extensive research aiming at combining efficient methods of structural analysis with stochastic analysis, where the influence of random variables is thoroughly evaluated.

The only method that has become widespread in engineering design practice is the Monte Carlo simulation technique. Probabilistic design parameters are sampled and a number of deterministic computations are performed to provide information about the distribution, or some statistics of response parameters. This is an accurate and simple approach, but also very expensive in terms of computer resources. Several methods that could be employed at a lower computational cost have been proposed. These can be divided into three main categories. One od these methods concern the sampling itself of the Monte Carlo technique in order to reduce the number of realizations required to provide reliable statistics of the response. To this category belong stratified sampling and Latin hypercube sampling.

In stochastic simulations the variables can be of two kinds, variables with uncertain properties and variables with design properties. The uncertain variables are those that actually are uncertain due to various kinds of imperfections or varying production tolerances, whereas free design parameters are used to create some sort of optimal solution. Both of these must be treated in a design case and most production parameters inherently contain them both.

2.4 Latin Hypercube Sampling

In order to reduce the required number of realizations, Latin hypercube sampling can be employed. As for the SMC method, the desired accuracy in the estimated distribution function determines the required number of realizations. Let n denote the required number of realizations and k the number of random variables. The sampling space is then k-dimensional. An $n \times k$ matrix $\mathbf{P}$, in which each of the k columns is a random permutation of (1,n), and an $n \times k$ matrix $\bar{\mathbf{R}}$ of independent random numbers from the uniform (0,1) distribution are established. Then the elements of the sampling matrix $\bar{\mathbf{V}}$ are determined

as

$$\bar{V}_{ij} = F_j^{-1}\left(\frac{P_{ij} - \bar{R}_{ij}}{n}\right) \tag{21}$$

where F_j^{-1} represents the inverse of the target cumulative distribution function for variable j. Each row in $\bar{\mathbf{V}}$ now contains input for one deterministic computation. For two input variables and five realizations, a possible sampling plan is shown in figure 1. Note that the sample is spread over the entire sampling space as the generation of the Latin hypercube sampling plan requires one image from each row and each column. If n realizations from the entire sampling space had been chosen completely at random, as in SMC sampling, there is a risk that they would form a cluster and some parts of the sampling space would not be investigated.

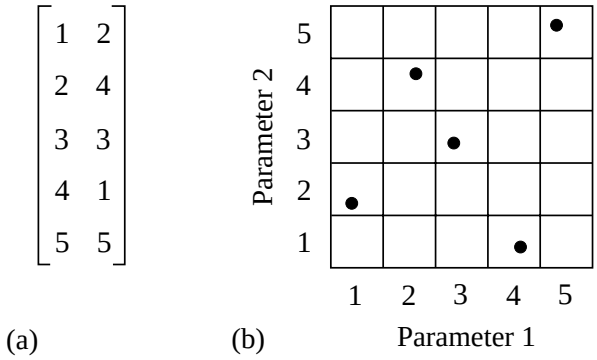

Figure 1: Latin cube, two variables and five realizations. The 5×2 matrix (a) determines the plan illustrated in (b).

Even though the marginal distribution of each variable is efficiently represented, there is a risk that some spurious correlation appears, see figure 2(a). However, such spurious correlation can be reduced by modifications in the permutation matrix **P**, see figure 2(b).

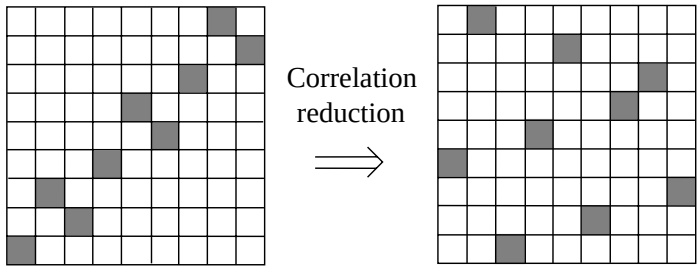

Figure 2: Spurious correlation of sampling plan (a) is reduced in plan (b).

3 Application examples

The following application examples are intended to show how the described theories can be used. A standard finite element analysis of a acoustic cavity is a procedure in many applications, such as passenger compartments in automobiles and aircrafts. The method is not so well spread in room acoustical situations. One reason is tradition, the finite element method has not been a well accepted method in acoustics. Another reason could be that the validity of the finite element method in room acoustic analysis is only up to a certain frequency limit, say 500 Hz. On the other hand, more traditional acoustic methods are not well suited for low frequency analysis, they need a high mode density. Also many traditional acoustic methods are analytically, and can only deal with problems that have certain boundary conditions. Therefore, in practical situations, with complex geometry and complex topology, these methods are not applicable.

3.1 Room with flexible gypsum wall.

The first example is a very simple case of a rectangular room where damping material is placed at different locations on the boundary surface. The system is excited by a point source representing a loudspeaker, see figure 3. The influence of the placement of absorbtion material on the sound pressure level is studied. In figure 4 the sound pressure levels measured in the shaded area of figure 3 accomplished by the point source when one wall at a time is totally covered with damping material is seen.The damping material is modelled as a porous sound absorbing material described in section 2.2 . This shows the possibility to control the sound pressure field by introducing damping material.

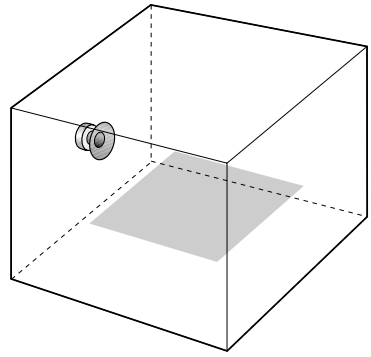

Figure 3: *Test case, rectangular room with loudspeaker.*

The results from the analysis could also be seen in a snapshot plot of the pressure distribution in the room at a certain frequency. Figure 5 shows the pressure distribution for one frequency at two height levels in the room. This could be very useful, if e.g. you are interested of the sound comfort at a certain position in a room, and by viewing at the results in

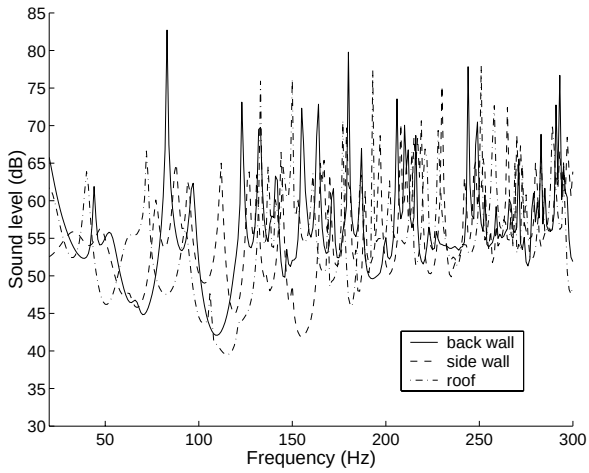

Figure 4: *Frequency response for different damper locations.*

such a detailed way, new insights can be made about the sound level at a certain position in the room.

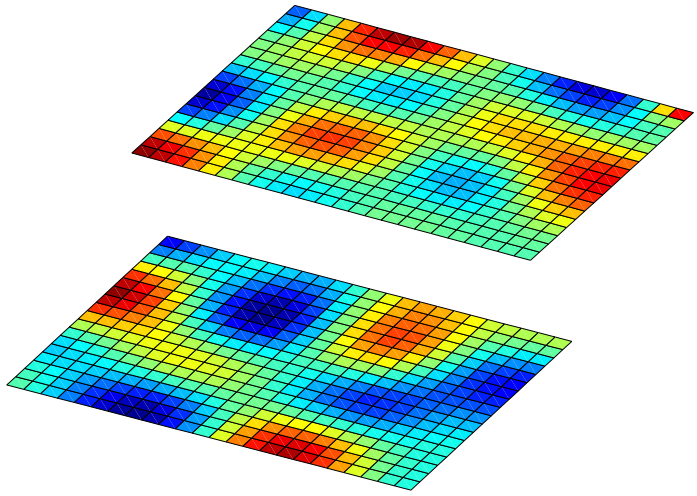

Figure 5: *Frequency response for one damper location at to hight levels in the room.*

The purpose of this example was just to show that the use of the finite element method gives large possibilities to view and analyse the result. It gives both the possibility to plot e.g. sound pressure level against frequency, but also view the pressure distribution anywhere in the space of the room.

3.2 Room with stochastic variation in size and damper material properties

The second example is the same room again with dimensions according to figure 6.

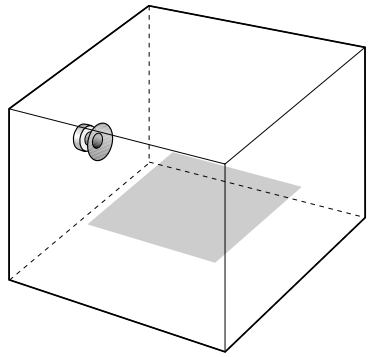

Figure 6: *Rectangular room with loudspeaker. Room width is 3.6 m, height 2.4 m and length is 4.8 m.*

In this case the room length has probabilistic value, where the mean value was chosen to 4.8 m and the standard deviation to 0.2. Dampers are placed on the backwall in this case, and the material properties of the dampers was also given a stochastic variation with a mean value of porosity of 2500 and a standard deviation of 2000. An analysis procedure is created with the LHS routines and in this case 20 simulations were setup for the analysis.

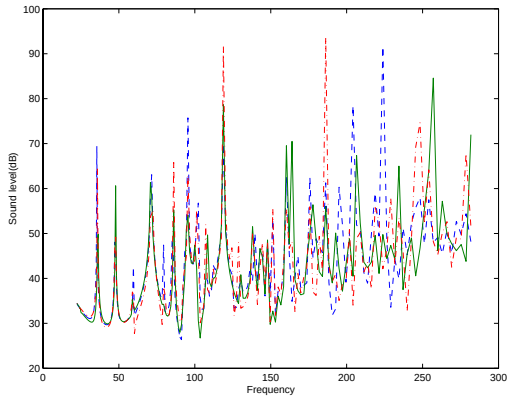

Figure 7: *Frequency response from three different stochastic configurations*

Figure 7 shows frequency response from three different stochastic configurations. As can be seen there are differences in the results at some points, although the stochastic variation has been quite small.

Figure 8 shows pressure response for different frequencies and different heights in the room. The figure shows the sound pressure level in the shaded area in figure 6 for three different stochastic combinations.

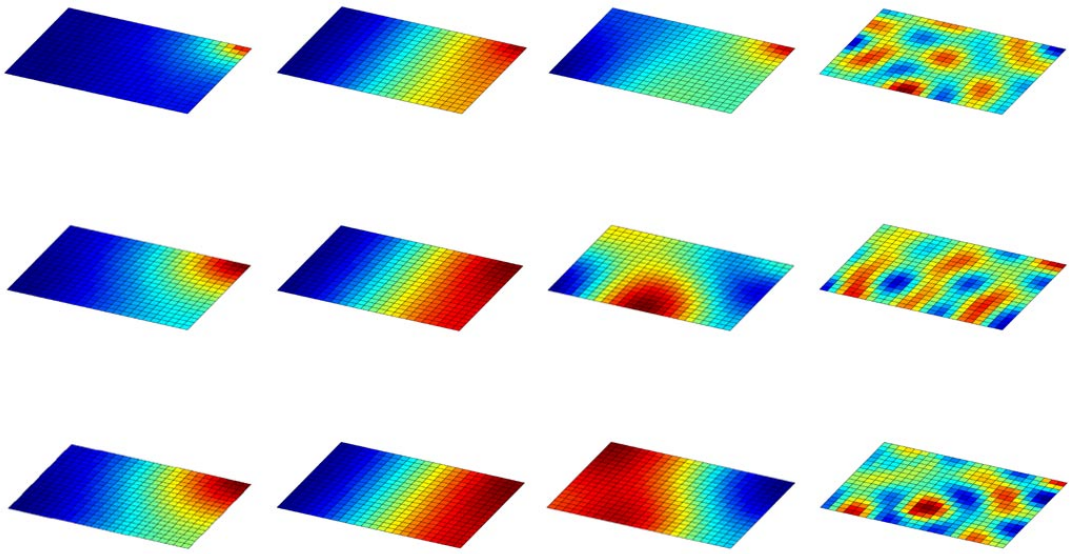

Figure 8: *Frequency response for different damper locations and room lengths. Going from left to right are response for frequencies 22 Hz, 34 Hz, 77 Hz and 199 Hz. The first row are responses at 2.0 m above the floor, the second row for 1.2 m and the last row for 0.4 m.*

The spatial averages of the sound pressure level, filtered into $\frac{1}{3}$-octave bands can be calculated as where

$$L_i^{f_a - f_b} = 10 \log \left(\sum_{f=f_a}^{f_b} 10^{L_i/10} \right) \tag{22}$$

As can be seen in figure 9 the results from different simulations can be quit different. From the results one can find maximum and minimum responses due to different stochastic configurations.

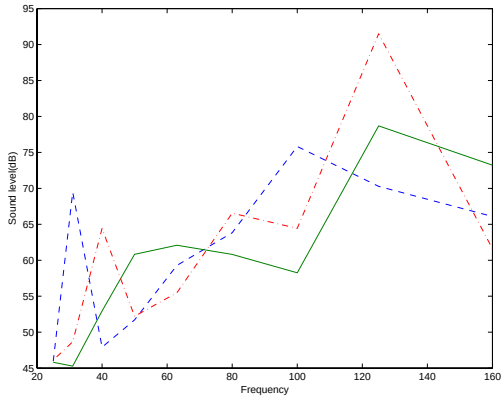

Figure 9: *Sound pressure level for three different stochastic configurations*

3.3 Room with stochastic variation in position of chairs

In this case the room has been occupied by some furniture. Two chairs are randomly positioned in the room. The position of the chair is the stochastic variable. The chairs are made of a material the has a damping effect and is modelled in the same way as in previous example. The material properties also have a stochastic variation.

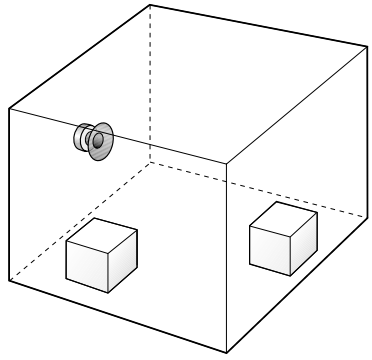

Figure 10: *Rectangular room with loudspeaker. Room width is 3.6 m, height 2.4 m and length is 4.8 m. Two chairs positioned with stochastic variation*

In figure 11 the results from three different set of furniture positions are shown.

4 Discussion

In a number of application examples the usability of finite element analysis in rooms acoustical situations has been demonstrated. The analysis was made in combination with

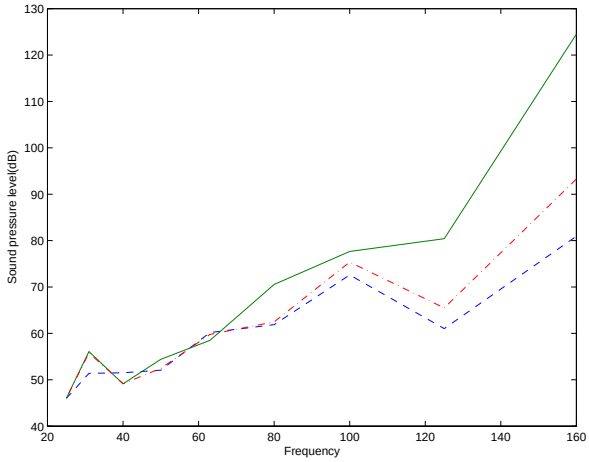

Figure 11: *Sound pressure level for three different stochastic configurations*

a stochastic simulation technique, Latin hypercube sampling. The intension was to show that the finite element method could be a useful design instrument in room acoustical situations. The influence of variation in e.g. geometry or material properties could easily be studied in the design phase, at a low cost. There are a number of situations where similar analysis could be conducted:

- Simulation of sound insulation in building acoustics. In a paper by Davidsson *et el* [10] sound transmission loss for different double-leaf walls were studied. The influence of several parameters were investigated, e.g. the density of the plaserboard, different geometries of the wall studs and variation of the porous material density of sound insulating material in the wall. Other situations where this could be used is e.g. investigation of sound insulation of windows.

- Simulation of loudspeaker placement in a room. When tuning a hifi equipment so that the best possible performance is achieved, an analysis of the placement of the loudspeakers with regard to the listening position could be conducted.

- Design of room dimensions for critical listening environments. In e.g. [11] the author tries to optimize the shape of a room. The goal is to achieve a smoother sound pressure distribution in the low frequency range.

- General modelling of sound fields in building environments, taking uncertainties into account.

To improve the usability of the suggested method, there are a number of things to be done:

- Better material models of damping materials are needed in the implementations. In e.g. [12] Biot's material models are described that could be used in room acoustical analysis as well.

- A software implementation that are intended to be used by a person who not necessarily is a finite element expert. At least the stochastic routines should be packaged in a more user friendly way. The goal should be that the results from these calculations should be easier to visualise and interpret.
- Implement the best possible reduction techniques to be able to run larger problem sizes, i.e. be able to analyse the problems at higher frequencies.
- Create a toolbox in the software that immediately can calculate traditional acoustic measures, such as reverbation time and sound transmission loss.
- Implement a simple stochastic optimisation routine. Such a routine is not intended to find the optimal solution to a problem. On the contrary, an acceptable goal is set up for a number of variables, and then the solution is accepted when the goal is achieved.

References

[1] W. C. Sabine, *Collected papers on acoustics*, Dover publications, 3–42, (1964).

[2] Philip M. Morse and Herman Feshbach, *Methods of Theoretical Physics*, McGraw-Hill, New York, (1953).

[3] A. Craggs, The use of simple 3-D acoustic elements for determining natural frequencies of complex shaped cavities, *J. Sound Vib*, **23**, 331–339, (1972).

[4] P.M Petyt, J. Leas amd G.H. Koopman, A finite element method for determining the acoustic modes of irregular shapes, *J. Sound Vib*, **45**, 495–502, (1976).

[5] G. Sandberg, P-A. Hansson, M. Gustavsson, Domain Decomposition in Acoustic and Structure-Acoustic Analysis, *Computer methods in applied mechanics and engineering*, **190**, 2979–2988, (2001).

[6] J. F. Allard, *Propagation of sound in porous media; modelling sound absorbing matarials*, McGraw-Hill, London, Fourth edition, (1989).

[7] O.C. Zienkiewicz and R.L. Taylor, *The Finite Element Method*, Elsevier Science Publishers Ltd, (1993).

[8] V. Martin and A. Brodrero, An introduction to the control of sound fields by optimising impedance locations on the wall of an acoustic cavity, *Journal of Sound and Vibration*, **204**, 331–357, (1997).

[9] V. Easwaran and A. Craggs, On further validation and use of the finite element method to room acoustics, *Journal of Sound and Vibration*, **187**, 195–212, (1995).

[10] P. Davidsson, J. Brunskog, P-A. Wernberg, G. Sandberg and P. Hammer, Analysis of sound transmission loss of double-leaf walls in the low-frequency range using the finite element method, *Building Acoustics*, **11**, 239–257(2004)

[11] C. Papadopoulos, Redistribution of the low frequency acoustic modes of a room: a finite element-based optimisation method, *Applied Acoustics*, **62**, 1267-1285(2001)

[12] P. Davidsson, Structure-Acoustic Analysis;Finite Element Modelling and Reduction Methods, Pdh Thesis, Report TVSM-1018, Lund (2004)

[13] A Olssson, Probabilistic Analysis and reliability of engineering structures, Pdh Thesis, Report TVSM-1014, Lund (2002)

[14] G. Sandberg, G. Kjell and J. de Mare, Computational planning using Latin hyper-cube sampling, *Report TVSM-7118*, Division of Structural Mechanics, Lund Univerity(1996)